frequency where the phase reaches -2π radians (which we define as f_0), oscillations of AP and SNA will occur at around f_0. In our actual data, f_0 was approximately 0.13 Hz (Fig. 3*E*), which is consistent with a previous study (Malpas & Burgess, 2000) showing increased 0.1 Hz oscillation of AP during haemorrhage in rabbits. Moreover, the gain at f_0 was less than 1 (Fig. 3*E*), indicating no oscillations generated according to the baroreflex loop theory. Therefore, in the closed-loop-spontaneous condition, the baroreflex loop theory would not contribute to the 0.4 Hz fluctuations of AP and SNA.

Lastly, respiratory-mediated fluctuation of AP may contribute to SNA fluctuation via baroreflex mechanisms. In the baroreflex open-loop condition (Fig. 3*B*), SNA autospectrum shows no peak whereas systemic AP shows a large peak at the frequency of artificial respiration (approximately 0.57 Hz) (Fig. 3*B*). This indicates that AP fluctuation at that frequency is not mediated by SNA but by mechanical aspects of respiration (i.e. respiratory changes in intrathoracic pressure), consistent with an earlier report (Brychta *et al.* 2007). Since closing the baroreflex loop produces a peak in the SNA autospectrum at the respiratory frequency (Fig. 4*B*), a baroreflex mechanism may partly be responsible for respiratory-mediated SNA fluctuation in this experimental condition.

Physiological implication (3): open-loop baroreflex neural arc transfer function is able to predict closed-loop time-series SNA response to drug-induced AP change

The data discussed so far were obtained using mechanical interventions to change carotid sinus pressure, which arguably are not physiological changes. To validate whether the predictabilities of the open-loop and closed-loop-spontaneous transfer functions apply to more physiological conditions, we tested the neural arc transfer functions using pharmacological pressure intervention (phenylephrine and nitroprusside infusions) under closed-loop conditions. First, the SNA predicted by the open-loop baroreflex neural arc transfer function ($H_{\text{n-open}}$) in response to the measured changes in CSP (= AP) was roughly similar to the actually measured SNA with respect to both amplitude and timing of neural activity (Fig. 10*A*, third and fourth panel), showing high correlation ($r^2 = 0.9$, Fig. 10*B*). This result indicates that with regard to the neural arc, the open-loop transfer function is able to predict time-series SNA output from AP input even during pharmacological pressure interventions. A possible explanation for the good predictability is that since the pharmacological interventions exert a noise to the peripheral and not the neural arc, time-series SNA is almost determined by the pharmacologically induced changes in baroreceptor pressure (= systemic AP) via the neural arc transfer function (= $H_{\text{n-open}}$).

In contrast to the open-loop transfer function, the SNA predicted by the closed-loop-spontaneous baroreflex neural arc transfer function ($H_{\text{n-closed-spon}}$) was different from the measured SNA. The predicted SNA was an oppositely directed neural response: when AP (= CSP) increased, the predicted SNA increased whereas the measured SNA decreased, and vice versa. Therefore, with regard to the neural arc, the closed-loop-spontaneous transfer function is not able to predict SNA dynamics from AP. The failure in predicting SNA change may be explained by inappropriate system identification in the closed-loop condition. Because of the closed-loop condition, the calculated phase function of $H_{\text{n-closed-spon}}$ was the inverse of that of $H_{\text{p-closed-spon}}$. Indeed, the phase led as frequency increased (Figs 5, 11*B* and *D*) in contrast to the phase lag of the open-loop transfer function ($H_{\text{n-open}}$). Furthermore, the calculated phase of $H_{\text{n-closed-spon}}$ resulted in an oppositely directed response of predicted SNA as compared with actually measured SNA, in contrast to the good match of predicted SNA by $H_{\text{n-open}}$. These results indicate that with regard to the neural arc, the open-loop neural arc transfer function predicts time-series SNA response to changes in AP induced by pharmacological interventions, while the closed-loop-spontaneous transfer function cannot predict SNA response.

Although spontaneous baroreflex measures are believed to represent the neural arc function (baroreflex control of SNA), the present study raises potential methodological issues. First, since the baroreflex is a closed-loop feedback system, there is theoretical difficulty in identifying system characteristics in the closed-loop spontaneous condition. Since a relationship calculated from SNA input to AP during their spontaneous fluctuations is the inverse of that calculated from AP input to SNA, the calculation itself cannot determine the causality between them. Our present data clearly indicate limitation in estimating closed-loop-spontaneous transfer function of the neural arc, and that a good estimation requires opening the loop and introducing an intervention to the loop. Furthermore, although the spontaneous baroreflex transfer function obtained in the closed-loop condition (Orea *et al.* 2007; Cooke *et al.* 2009; Ogoh *et al.* 2009) has been used as a surrogate for the neural (feedback) arc function of the baroreflex loop, it actually represents the peripheral (feedforward) arc function since baroreflex loop is predominantly feedforward rather than feedback in the closed-loop-spontaneous condition.

Second, a recent study (Hart *et al.* 2010) has reported that spontaneous baroreflex measures (slope of strength of muscle SNA burst over-binned or non-binned AP) did not correlate ($r^2 = 0.05$–0.13) with the 'gold standard' modified Oxford analysis (nitroprusside and phenylephrine), whereas spontaneous threshold measure

(slope of % occurrence of muscle SNA burst over 1 mmHg binned AP, eliminating strength of SNA burst) correlated with it mildly ($r^2 = 0.5$). Although we cannot directly compare the transfer function analysis in our present study with the spontaneous threshold measure reported by Hart *et al.* (2010) because of methodological differences, our open-loop transfer function of the neural arc was able to predict occurrence and magnitude of time-series SNA with a higher degree of accuracy ($r^2 = 0.9$, Fig. 10*B*) and reproduce the AP–SNA relationship during closed-loop, drug-induced AP changes (Fig. 10*D*).

Limitations

The present study has several limitations. First, we excluded the efferent effect of the vagally mediated arterial baroreflex, which could affect the properties of baroreflex control of SNAs. Second, artificial respiration and surgical procedures used in this study could affect baroreflex. Third, anaesthetic agents tend to inhibit efferent SNA and depress the gain of baroreflex control of SNA. Fourth, since the present study was animal research, it is limited in its applicability to humans. However, a problem of difficulty in identifying the 'closed-loop' system in contrast with the 'open-loop' system is common in animal and human studies. Lastly, we perfused the carotid sinuses with physiological saline pre-equilibrated with atmospheric. Local hypoxia could have occurred and somewhat affected baroreflex control of SNA. Further research to examine the relevance of the present findings to true physiological conditions is necessary.

Summary

In summary, the open-loop baroreflex transfer functions for the neural and peripheral arcs allowed good prediction of the time-series SNA and AP outputs from baroreceptor pressure and SNA inputs, respectively. In contrast, the closed-loop-spontaneous baroreflex transfer function for the neural arc deviated greatly from the open-loop transfer function, and could not predict the time-series SNA dynamics. However, the closed-loop-spontaneous baroreflex transfer function for the peripheral arc partially matched the open-loop transfer function, with reasonable predictability of the time-series AP dynamics although slightly inferior in accuracy. Furthermore, the predictabilities of open-loop and closed-loop-spontaneous transfer functions of the neural arc were validated by closed-loop pharmacological (phenylephrine and nitroprusside infusions) pressure interventions. Time-series SNA responses to drug-induced AP changes predicted by the open-loop transfer function matched closely the measured responses, whereas SNA responses predicted by the closed-loop-spontaneous transfer function deviated greatly and were the inverse of measured responses. Therefore, although the spontaneous baroreflex transfer function obtained by closed-loop analysis has been believed to represent the neural arc function, it is inappropriate for system identification of the neural arc but is partially appropriate for system identification of the peripheral arc under resting condition, compared with open-loop analysis.

Appendix A

In a block diagram of the open-loop baroreflex system (Fig. 1*A*), CSP is independent of systemic AP because of vascular isolation of the carotid-sinus regions. In this framework, input–output relationships of these arcs are expressed in the frequency domain as:

$$\mathrm{SNA}(f) = H_\mathrm{n}(f) \cdot \mathrm{CSP}(f) + \mathrm{NN}(f) \quad \text{(A1)}$$

$$\mathrm{AP}(f) = H_\mathrm{p}(f) \cdot \mathrm{SNA}(f) + \mathrm{PN}(f) \quad \text{(A2)}$$

where CSP(f), SNA(f) and AP(f) are the fast Fourier transforms of CSP, SNA and systemic AP, respectively. $H_\mathrm{n}(f)$ and $H_\mathrm{p}(f)$ denote the neural arc and the peripheral arc transfer functions, respectively. NN(f) and PN(f) represent unknown noise in the neural and peripheral arcs, respectively.

In the neural arc, calculating the ensemble averages of cross-powers between the terms of eqn (A1) and CSP(f) yields

$$E[\mathrm{SNA}(f) \cdot \mathrm{CSP}(f)^*] = H_\mathrm{n}(f) \cdot E[\mathrm{CSP}(f) \cdot \mathrm{CSP}(f)^*] + E[\mathrm{NN}(f) \cdot \mathrm{CSP}(f)^*] \quad \text{(A3)}$$

where $E[\,]$ indicates an ensemble average operation. CSP(f)* denotes the complex conjugate of CSP(f). As $H_\mathrm{n}(f)$ is supposed to be time invariant during the observation period, $H_\mathrm{n}(f)$ is outside the ensemble average operation. When CSP is a white-noise signal, E[NN(f)·CSP(f)*] diminishes to zero asymptotically because the white noise is statistically independent of any other noise signal. Thus, we can estimate $H_\mathrm{n}(f)$ by the following equation, which we designate $H_{\text{n-open}}(f)$.

$$H_\mathrm{n}(f) = \frac{E[\mathrm{SNA}(f) \cdot \mathrm{CSP}(f)^*]}{E[\mathrm{CSP}(f) \cdot \mathrm{CSP}(f)^*]} = H_{\text{n-open}}(f) \quad \text{(A4)}$$

Similarly, in the peripheral arc, calculating ensemble averages of cross-powers between terms of eqn (A2) and SNA(f) yields

$$E[\mathrm{AP}(f) \cdot \mathrm{SNA}(f)^*] = H_\mathrm{p}(f) \cdot E[\mathrm{SNA}(f) \cdot \mathrm{SNA}(f)^*] + E[\mathrm{PN}(f) \cdot \mathrm{SNA}(f)^*] \quad \text{(A5)}$$

where SNA(f)* denotes the complex conjugate of SNA(f). As $H_\mathrm{p}(f)$ is supposed to be time invariant during the

observation period, $H_p(f)$ is outside the ensemble average operation. In the open-loop condition, since PN(f) cannot affect SNA(f) and is statistically independent of SNA(f) by definition, E[PN(f)·SNA(f)*] diminishes to zero asymptotically. Thus, we can estimate $H_p(f)$ by the following equation, which we designate $H_{p\text{-open}}(f)$.

$$H_p(f) = \frac{E[\mathrm{AP}(f) \cdot \mathrm{SNA}(f)^*]}{E[\mathrm{SNA}(f) \cdot \mathrm{SNA}(f)^*]} = H_{p\text{-open}}(f) \quad \text{(A6)}$$

In contrast to the open-loop condition, CSP is matched with systemic AP in the closed-loop-spontaneous baroreflex condition (Fig. 1*B*). Thus, the input–output relationships of the arcs in the frequency domain are expressed as:

$$\mathrm{SNA}(f) = H_n(f) \cdot \mathrm{AP}(f) + \mathrm{NN}(f) \quad \text{(A7)}$$

$$\mathrm{AP}(f) = H_p(f) \cdot \mathrm{SNA}(f) + \mathrm{PN}(f) \quad \text{(A8)}$$

In the neural arc, calculating ensemble averages of cross-powers between the terms of eqn (A7) and AP(f) yields

$$E[\mathrm{SNA}(f) \cdot \mathrm{AP}(f)^*] = H_n(f) \cdot E[\mathrm{AP}(f) \cdot \mathrm{AP}(f)^*] + E[\mathrm{NN}(f) \cdot \mathrm{AP}(f)^*] \quad \text{(A9)}$$

$$H_n(f) = \frac{E[\mathrm{SNA}(f) \cdot \mathrm{AP}(f)^*]}{E[\mathrm{AP}(f) \cdot \mathrm{AP}(f)^*]} - \frac{E[\mathrm{NN}(f) \cdot \mathrm{AP}(f)^*]}{E[\mathrm{AP}(f) \cdot \mathrm{AP}(f)^*]} \quad \text{(A10)}$$

However, in the baroreflex closed-loop conditions, the unknown noise in SNA (NN) can affect AP through the peripheral arc transfer function (H_p). In other words, AP(f) inevitably correlates with NN(f), and E[NN(f)·AP(f)*] does not diminish to zero. $H_n(f)$ cannot be determined because the unknown noise NN is practically impossible to quantify. Therefore in protocol 3, we simplify eqn (A10) by neglecting the last term, and define the closed-loop-spontaneous transfer function by the following equation, which we designate $H_{n\text{-closed-spon}}(f)$.

$$H_n(f) = \frac{E[\mathrm{SNA}(f) \cdot \mathrm{AP}(f)^*]}{E[\mathrm{AP}(f) \cdot \mathrm{AP}(f)^*]} = H_{n\text{-closed-spon}}(f) \quad \text{(A11)}$$

However, from eqns (A4) and (A11), it is evident that $H_{n\text{-closed-spon}}(f)$ should be different from $H_{n\text{-open}}(f)$ when NN(f) is large and cannot be neglected.

In the peripheral arc, calculating ensemble averages of cross-powers between the terms of eqn (A8) and SNA(f) yields:

$$E[\mathrm{AP}(f) \cdot \mathrm{SNA}(f)^*] = H_p(f) \cdot E[\mathrm{SNA}(f) \cdot \mathrm{SNA}(f)^*] + E[\mathrm{PN}(f) \cdot \mathrm{SNA}(f)^*] \quad \text{(A12)}$$

$$H_p(f) = \frac{E[\mathrm{AP}(f) \cdot \mathrm{SNA}(f)^*]}{E[\mathrm{SNA}(f) \cdot \mathrm{SNA}(f)^*]} - \frac{E[\mathrm{PN}(f) \cdot \mathrm{SNA}(f)^*]}{E[\mathrm{SNA}(f) \cdot \mathrm{SNA}(f)^*]} \quad \text{(A13)}$$

However, in the baroreflex closed-loop conditions, the unknown noise in AP (PN) can affect SNA through the neural arc transfer function (H_n). In other words, SNA(f) inevitably correlates with PN(f), and E[PN(f)·SNA(f)*] does not diminish to zero. $H_p(f)$ cannot be determined because the unknown noise PN is practically impossible to quantify. Therefore in protocol 3, we simplify eqn (A13) by neglecting the last term and define the closed-loop-spontaneous transfer function by the following equation, which we designate $H_{p\text{-closed-spon}}(f)$.

$$H_p(f) = \frac{E[\mathrm{AP}(f) \cdot \mathrm{SNA}(f)^*]}{E[\mathrm{SNA}(f) \cdot \mathrm{SNA}(f)^*]} = H_{p\text{-closed-spon}}(f) \quad \text{(A14)}$$

However, from eqns (A6) and (A14), it is evident that $H_{p\text{-closed-spon}}(f)$ should be different from $H_{p\text{-open}}(f)$ when PN(f) is large and cannot be neglected.

Appendix B

In rabbits, the transfer function of the baroreflex neural arc (baroreceptor pressure/CSP to SNA) approximates derivative characteristics in the frequency range below 0.8 Hz, and high-cut characteristics of frequencies above 0.8 Hz (Kawada *et al.* 2002). Therefore, according to our previous study, we model the neural arc transfer function (H_n) using eqn (B1) as follows

$$H_n(f) = -K_n \frac{1 + \frac{f}{f_{c1}} j}{\left(1 + \frac{f}{f_{c2}}\right)^2} \exp(-2\pi f j L) \quad \text{(B1)}$$

where f and j represent the frequency (in Hz) and imaginary units, respectively; K_n is static gain (in a.u. mmHg^{-1}); f_{c1} and f_{c2} ($f_{c1} < f_{c2}$) are corner frequencies (in Hz) for derivative and high-cut characteristics, respectively; and L is a pure delay (in s), that would represent the sum of delays in synaptic transmission in the baroreflex central pathways and the sympathetic ganglion. The dynamic gain increases in the frequency range from f_{c1} to f_{c2}, and decreases above f_{c2}. Based on the measured results, we set K_n, f_{c1}, f_{c2} and L at 1, 0.1, 0.8 and 0.2, respectively, in all simulations in Fig. 11.

In addition, the transfer function of the baroreflex peripheral arc (SNA to systemic AP) approximates the second-order low-pass filter with a lag time in rabbits (Kawada *et al.* 2002). Therefore, we model the peripheral

arc transfer function (H_p) using eqn (B2) as follows:

$$H_p(f) = \frac{K_p}{1 + 2\zeta\frac{f}{f_N}j + \left(\frac{f}{f_N}j\right)^2} \exp(-2\pi f j L) \quad \text{(B2)}$$

where K_p is static gain (in mmHg a.u.$^{-1}$); fN and ζ indicate a natural frequency (in Hz) and a damping ratio, respectively; and L is a pure delay (in s) that would represent the sum of delays in synaptic transmission in the neuroeffector junction and intracellular signal transduction in the effector organs. Based on the measured results, we set K_p, f_N, ζ and L at 1, 0.07, 1.4 and 1.0, respectively, in all simulations in Fig. 11.

References

Barres C, Cheng Y & Julien C (2004). Steady-state and dynamic responses of renal sympathetic nerve activity to air-jet stress in sinoaortic denervated rats. *Hypertension* **43**, 629–635.

Brychta RJ, Shiavi R, Robertson D, Biaggioni I & Diedrich A (2007). A simplified two-component model of blood pressure fluctuation. *Am J Physiol Heart Circ Physiol* **292**, H1193–H1203.

Cooke WH, Hoag JB, Crossman AA, Kuusela TA, Tahvanainen KU & Eckberg DL (1999). Human responses to upright tilt: a window on central autonomic integration. *J Physiol* **517**, 617–628.

Cooke WH, Rickards CA, Ryan KL, Kuusela TA & Convertino VA (2009). Muscle sympathetic nerve activity during intense lower body negative pressure to presyncope in humans. *J Physiol* **587**, 4987–4999.

deBoer RW, Karemaker JM & Strackee J (1987). Hemodynamic fluctuations and baroreflex sensitivity in humans: a beat-to-beat model. *Am J Physiol Heart Circ Physiol* **253**, H680–H689.

DiBona GF & Sawin LL (2003). Frequency response of the renal vasculature in congestive heart failure. *Circulation* **107**, 2159–2164.

DiBona GF & Sawin LL (2004). Effect of renal denervation on dynamic autoregulation of renal blood flow. *Am J Physiol Renal Physiol* **286**, F1209–F1218.

Drummond GB (2009). Reporting ethical matters in *The Journal of Physiology*: standards and advice. *J Physiol* **587**, 713–719.

Eckberg DL & Sleight P (1992). *Human Baroreflexes in Health and Disease*. Oxford University Press, New York.

Guyton A & Harris J (1951). Pressoreceptor-autonomic oscillation: a probable cause of vasomotor waves. *Am J Physiol* **165**, 158–166.

Hart EC, Joyner MJ, Wallin BG, Karlsson T, Curry TB & Charkoudian N (2010). Baroreflex control of muscle sympathetic nerve activity: a nonpharmacological measure of baroreflex sensitivity. *Am J Physiol Heart Circ Physiol* **298**, H816–H822.

Ikeda Y, Kawada T, Sugimachi M, Kawaguchi O, Shishido T, Sato T *et al.* (1996). Neural arc of baroreflex optimizes dynamic pressure regulation in achieving both stability and quickness. *Am J Physiol Heart Circ Physiol* **271**, H882–H890.

Ikeda Y, Sugimachi M, Yamasaki T, Kawaguchi O, Shishido T, Kawada T *et al.* (1995). Explorations into development of a neurally regulated cardiac pacemaker. *Am J Physiol Heart Circ Physiol* **269**, H2141–H2146.

Julius SB & Allan GP (ed.) (2000). *Random Data: Analysis and Measurement Procedures*. John Wiley & Sons, Inc., New York.

Kamiya A, Hayano J, Kawada T, Michikami D, Yamamoto K, Ariumi H *et al.* (2005*a*). Low-frequency oscillation of sympathetic nerve activity decreases during development of tilt-induced syncope preceding sympathetic withdrawal and bradycardia. *Am J Physiol Heart Circ Physiol* **289**, H1758–H1769.

Kamiya A, Kawada T, Mizuno M, Shimizu S & Sugimachi M (2010). Parallel resetting of arterial baroreflex control of renal and cardiac sympathetic nerve activities during upright tilt in rabbits. *Am J Physiol Heart Circ Physiol* **298**, H1966–H1975.

Kamiya A, Kawada T, Yamamoto K, Michikami D, Ariumi H, Miyamoto T *et al.* (2005*b*). Dynamic and static baroreflex control of muscle sympathetic nerve activity (SNA) parallels that of renal and cardiac SNA during physiological change in pressure. *Am J Physiol Heart Circ Physiol* **289**, H2641–H2648.

Kamiya A, Kawada T, Yamamoto K, Mizuno M, Shimizu S & Sugimachi M (2008*a*). Upright tilt resets dynamic transfer function of baroreflex neural arc to minify the pressure disturbance in total baroreflex control. *J Physiol Sci* **58**, 189–198.

Kamiya A, Michikami D, Iwase S & Mano T (2008*b*). Decoding rule from vasoconstrictor skin sympathetic nerve activity to nonglabrous skin blood flow in humans at normothermic rest. *Neurosci Lett* **439**, 13–17.

Kawada T, Li M, Kamiya A, Shimizu S, Uemura K, Yamamoto H & Sugimachi M (2010). Open-loop dynamic and static characteristics of the carotid sinus baroreflex in rats with chronic heart failure after myocardial infarction. *J Physiol Sci* **60**, 283–298.

Kawada T, Zheng C, Yanagiya Y, Uemura K, Miyamoto T, Inagaki M *et al.* (2002). High-cut characteristics of the baroreflex neural arc preserve baroreflex gain against pulsatile pressure. *Am J Physiol Heart Circ Physiol* **282**, H1149–H1156.

Malpas SC & Burgess DE (2000). Renal SNA as the primary mediator of slow oscillations in blood pressure during hemorrhage. *Am J Physiol Heart Circ Physiol* **279**, H1299–H1306.

Ogoh S, Fisher JP, Young CN, Raven PB & Fadel PJ (2009). Transfer function characteristics of the neural and peripheral arterial baroreflex arcs at rest and during postexercise muscle ischemia in humans. *Am J Physiol Heart Circ Physiol* **296**, H1416–H1424.

Orea V, Kanbar R, Chapuis B, Barres C & Julien C (2007). Transfer function analysis between arterial pressure and renal sympathetic nerve activity at cardiac pacing frequencies in the rat. *J Appl Physiol* **102**, 1034–1040.

Rowell LB (1993). *Human Cardiovascular Control*. Oxford University Press, New York.

Zhang R, Zuckerman JH, Iwasaki K, Wilson TE, Crandall CG & Levine BD (2002). Autonomic neural control of dynamic cerebral autoregulation in humans. *Circulation* **106**, 1814–1820.

Author contributions

The experiments were performed at the Department of Cardiovascular Dynamics, National Cerebral and Cardiovascular Center Research Institute. A.K. absolutely contributed to: (1) Conception and design, (2) Collection, analysis and interpretation of data and (3) Drafting the article or revising it critically for important intellectual content. Other authors helped him particularly in (3). All authors approved the final version.

Acknowledgments

This study was supported by a research project promoted by Ministry of Health, Labour and Welfare in Japan (no. H21-nano-ippan-005, H22-nanchi-ippan-142), the Grants-in-Aid for Scientific Research promoted by Ministry of Education, Culture, Sports, Science and Technology in Japan (no. 20390462, 22791559) and the Industrial Technology Research Grant Program from New Energy and Industrial Technology Development Organization (NEDO) of Japan.

Am J Physiol Regul Integr Comp Physiol 300: R969–R977, 2011.
First published January 26, 2011; doi:10.1152/ajpregu.00768.2010.

Exercise training augments the dynamic heart rate response to vagal but not sympathetic stimulation in rats

Masaki Mizuno,[1,2] Toru Kawada,[2] Atsunori Kamiya,[2] Tadayoshi Miyamoto,[2,3] Shuji Shimizu,[2] Toshiaki Shishido,[2] Scott A. Smith,[1] and Masaru Sugimachi[2]

[1]*Departments of Physical Therapy and Internal Medicine, University of Texas Southwestern Medical Center at Dallas, Dallas, Texas;* [2]*Department of Cardiovascular Dynamics, National Cerebral and Cardiovascular Center Research Institute, Osaka, Japan; and* [3]*Department of Physical Therapy, Morinomiya University of Medical Sciences, Osaka, Japan*

Submitted 23 November 2010; accepted in final form 26 January 2011

Mizuno M, Kawada T, Kamiya A, Miyamoto T, Shimizu S, Shishido T, Smith SA, Sugimachi M. Exercise training augments the dynamic heart rate response to vagal but not sympathetic stimulation in rats. *Am J Physiol Regul Integr Comp Physiol* 300: R969–R977, 2011. First published January 26, 2011; doi:10.1152/ajpregu.00768.2010.—We examined the transfer function of autonomic heart rate (HR) control in anesthetized sedentary and exercise-trained (16 wk, treadmill for 1 h, 5 times/wk at 15 m/min and 15-degree grade) rats for comparison to HR variability assessed in the conscious resting state. The transfer function from sympathetic stimulation to HR response was similar between groups (gain, 4.2 ± 1.5 vs. 4.5 ± 1.5 beats·min^{-1}·Hz^{-1}; natural frequency, 0.07 ± 0.01 vs. 0.08 ± 0.01 Hz; damping coefficient, 1.96 ± 0.55 vs. 1.69 ± 0.15; and lag time, 0.7 ± 0.1 vs. 0.6 ± 0.1 s; sedentary vs. exercise trained, respectively, means ± SD). The transfer gain from vagal stimulation to HR response was 6.1 ± 3.0 in the sedentary and 9.7 ± 5.1 beats·min^{-1}·Hz^{-1} in the exercise-trained group ($P = 0.06$). The corner frequency (0.11 ± 0.05 vs. 0.17 ± 0.09 Hz) and lag time (0.1 ± 0.1 vs. 0.2 ± 0.1 s) did not differ between groups. When the sympathetic transfer gain was averaged for very-low-frequency and low-frequency bands, no significant group effect was observed. In contrast, when the vagal transfer gain was averaged for very-low-frequency, low-frequency, and high-frequency bands, exercise training produced a significant group effect ($P < 0.05$ by two-way, repeated-measures ANOVA). These findings suggest that, in the frequency domain, exercise training augments the dynamic HR response to vagal stimulation but not sympathetic stimulation, regardless of the frequency bands.

heart rate variability; transfer function; systems analysis

HEART RATE VARIABILITY (HRV) is considered to be a useful noninvasive assessment of autonomic nervous system activity. It has been well recognized that exercise training increases HRV at rest (4, 19). A recent meta-analysis by Sandercock et al. (28) demonstrated that exercise training results in significant increases in R-R interval and high-frequency (HF) power of HRV. Nevertheless, not all studies have demonstrated increases in HRV after exercise training (7). To date, the exact mechanisms underlying increases in HRV after exercise training remain to be elucidated. Many earlier studies have suggested that the augmentation of HRV induced by exercise training may be caused by a withdrawal of sympathetic tonus and/or an increase in vagal tonus (5, 14, 36). Autonomic tone assessed by HRV may reflect both the autonomic outflow from the central nervous system and the peripheral autonomic regulation of atrial pacemaker cells. The latter can be assessed quantitatively by examining the heart rate (HR) response to electrical stimulation of the autonomic nerves. Furthermore, recent studies suggested that peripheral autonomic regulation of atrial pacemaker cells could contribute to the exercise training-induced increases in cardiac vagal function (9, 10).

Equivocal results, however, have been reported using autonomic nerve stimulation. Regarding the vagal system, the effects of exercise training have been inconsistent among studies, showing both increases (9, 10) and reductions in vagally stimulated HR control (25). When considering the sympathetic system, a previous study demonstrated that the HR response to sympathetic stimulation was reduced by exercise training (22). However, the mechanisms underlying the training effect are controversial (3, 15, 26, 29, 33, 35). These equivocal results could be explained by differences in species and modes of exercise training among studies (i.e., exercise type, intensity, and duration, etc.). More importantly, since these studies of autonomic nerve stimulation did not evaluate HRV, a causal relationship between increased HRV and adaptation in peripheral autonomic HR control remains largely undetermined. Furthermore, despite the fact that HRV has been evaluated by using frequency domain as well as time domain analyses, to date, there are no reports available examining the effects of exercise training on the dynamic HR response to sympathetic or vagal stimulation in the frequency domain. Analysis of peripheral autonomic regulation in the frequency domain would advance our understanding of the mechanisms responsible for the alterations in HRV that occur in response to exercise training.

We have recently developed a technique to assess the dynamic characteristics of HR control by the autonomic nervous system in rats using transfer function analysis (21). The transfer function analysis can quantitatively evaluate the HR response to autonomic nerve stimulation over a wide frequency range that is necessary for interpreting the generation of HRV. Therefore, the aims of the present study were *1*) to identify the dynamic characteristics of sympathetic and vagal HR control in exercised-trained rats and *2*) to determine whether alterations in peripheral autonomic regulation contribute to changes in the frequency components of HRV in exercised-trained rats.

MATERIALS AND METHODS

Animal Care and Training Program

Animal care was in accordance with the "Guiding Principles for Care and Use of Animals in the Field of Physiological Sciences," approved by the Physiological Society of Japan. All protocols were reviewed and approved by the Animal Subjects Committee of the

Address for reprint requests and other correspondence: M. Mizuno, Dept. of Physical Therapy, Univ. of Texas Southwestern Medical Center at Dallas, 5323 Harry Hines Blvd., Dallas, TX 75390-9174 (e-mail: masaki.mizuno@utsouthwestern.edu).

National Cerebral and Cardiovascular Center. Fourteen male Sprague-Dawley rats (200–250 g body wt) were fed standard laboratory chow and water ad libitum and housed three per cage in a temperature-controlled room with a 12:12-h dark-light cycle. Rats were randomly assigned to one of two groups: sedentary ($n = 7$) and exercise trained ($n = 7$).

Exercise training was performed on a motor-driven treadmill, 5 days/wk for 16 wk, gradually progressing toward a speed of 15 m/min at a 15-degree grade for 60 min. Sedentary rats walked (10 m/min at 15 degrees) 10 min/day once per week during the 16-wk period to maintain treadmill familiarity. At the end of the 16-wk period, maximal exercise capacity was measured twice in each rat in tests separated by 2 days (6). The protocol for the maximal exercise capacity test consisted of walking at 10 m/min for 5 min followed by 2 m/min increases in speed every 2 min until the rat reached exhaustion. Rats were considered exhausted when they failed to stay off of a shock bar.

Assessment of Autonomic Tone in the Conscious Resting State

After the performance test, three steel electrodes were implanted under anesthesia. These electrodes were utilized for monitoring the electrocardiogram. The R-R interval was measured using a cardiotachometer (model AT601G; Nihon Kohden, Tokyo, Japan). On the first day of the study, which was 24 h after electrodes had been implanted, resting HR was recorded to analyze the R-R interval variability in the quiet unrestrained rat that was kept in a small box. In accordance with a previous study (25), autonomic tone was assessed by intraperitoneal injections of methylatropine (3 mg/kg) and propranolol (4 mg/kg). Immediately after resting HR was recorded, methylatropine was injected. Since the HR response to methylatropine reached its peak in 10–15 min, this time interval was allocated before the HR measurement. Propranolol was injected after methylatropine injection, and again the HR was measured after 10–15 min. Intrinsic HR was evaluated after simultaneous blockade by propranolol and methylatropine. Sympathetic tonus was defined as the difference between the HR after methylatropine injection and intrinsic HR. On the second day, propranolol was administered first to obtain the inverse sequence of blockade. Vagal tonus was defined as the difference between the HR after propranolol injection and intrinsic HR.

Sympathetic and Vagal Stimulation

Surgical preparations. After obtaining data for the assessment of autonomic tone and HRV, rats were anesthetized by a mixture of urethane (250 mg/ml) and α-chloralose (40 mg/ml), initiated with an intraperitoneal bolus injection of 1 ml/kg. If additional anesthesia was needed, 0.1 ml/kg was given intraperitoneally. The rats were intubated and mechanically ventilated with oxygen-enriched room air. The rats were slightly hyperventilated to suppress chemoreflexes. A catheter was placed in the right femoral artery and connected to a pressure transducer (model DX-200; Nihon Kohden, Tokyo, Japan) to measure arterial pressure (AP). HR was measured using a cardiotachometer (model AT601G; Nihon Kohden) triggered by the R wave on the electrocardiogram. A catheter was introduced into the right femoral vein for drug administration. Sinoaortic barodenervation was performed bilaterally to minimize changes in sympathetic efferent nerve activity via arterial baroreflexes. The vagi were sectioned bilaterally at the neck. A pair of bipolar stainless steel electrodes was attached to the right cervical sympathetic nerve for efferent sympathetic stimulation or the right cervical vagus for efferent vagal stimulation. The stimulation electrodes and nerve were secured with silicon glue (Kwik-Sil; World Precision Instruments, Sarasota, FL). Body temperature was monitored with a thermometer placed in the rectum and was maintained at 38°C with a heating pad throughout the experiment.

Experimental procedures. The pulse duration was set at 2 ms and the stimulation amplitude was fixed at 10 V for both sympathetic and vagal nerve stimulation. To allow for stabilization of hemodynamics, sympathetic and vagal nerve stimulations were started ~1 h after the end of surgical preparations. Between sympathetic and vagal stimulation protocols > 15 min elapsed to allow AP and HR to return to their respective baseline values.

To estimate the dynamic transfer characteristics from sympathetic stimulation to HR response, the sectioned end of the right cervical sympathetic nerve was stimulated employing a frequency-modulated pulse train for 10 min. The stimulation frequency was switched every 1,000 ms to either 0 or 5 Hz according to a binary white noise signal. The power spectrum of the stimulation signal was reasonably constant up to 0.5 Hz. The transfer function was estimated up to 0.5 Hz because the reliability of estimation decreased due to the diminution of input power above this frequency. The selected frequency range sufficiently spanned the range of physiological interest (21). For estimation of the static transfer characteristics from sympathetic stimulation to HR response, stepwise sympathetic stimulation was performed. Sympathetic stimulation frequency was increased from 1 to 5 Hz in 1-Hz increments. Each frequency step was maintained for 60 s.

To estimate the dynamic transfer characteristics from vagal stimulation to HR response, the right vagus was stimulated employing a frequency-modulated pulse train for 10 min. The stimulation frequency was switched every 500 ms to either 0 or 10 Hz according to a binary white noise signal. The power spectrum of the stimulation signal was reasonably constant up to 1 Hz. The transfer function was estimated up to 1 Hz because the reliability of estimation decreased due to the diminution of input power above this frequency. The selected frequency range sufficiently spanned the range of physiological interest (21). For estimation of the static transfer characteristics from vagal stimulation to HR response, stepwise vagal stimulation was performed. Vagal stimulation frequency was changed among 2, 4, 8, 16, and 32 Hz. Each frequency step was maintained for 60 s.

Data Analysis

Spectral analysis of HRV. Data obtained during the conscious resting state were digitized at 200 Hz utilizing a 12-bit analog-to-digital converter and stored on the hard disk of a dedicated laboratory computer system. Beat-by-beat time series of the R-R interval were interpolated every 130 ms (Δt). Twelve data segments of 512 (N) points overlapping half of the preceding data were processed. For each data segment, after the linear trend was removed and the Hanning window applied, power spectral density was computed using the fast Fourier transform algorithm. The frequency resolution was $\Delta f = 1/(N\,\Delta t)$, i.e., 0.015 Hz, and the highest frequency was $\Delta f = 1/2\Delta t$, i.e., 3.85 Hz, where f is frequency. The very-low-frequency (VLF) band ranged between 0.017 and 0.27 Hz, the low-frequency (LF) band between 0.27 and 0.75 Hz, and the high-frequency (HF) band between 0.75 and 3.3 Hz, according to an earlier report (8). The percentage of LF or HF power relative to the sum of LF and HF powers and the ratio of LF to HF power were also calculated.

Transfer function analysis. The dynamic characteristics of the HR response to sympathetic or vagal stimulation were estimated by a transfer function analysis (see APPENDIX for details). Dynamic sympathetic control of HR was quantified by fitting a second-order low-pass filter with pure delay to the estimated transfer function. The dynamic vagal control of HR was quantified by fitting a first-order, low-pass filter with pure delay to the estimated transfer function. To facilitate the intuitive understanding of the system's dynamic characteristics, we calculated the system step response of HR to 1-Hz nerve stimulation as follows.

The system impulse response was derived from the inverse Fourier transform of the transfer function. The system step response was then obtained from the time integral of the impulse response. The length of the step response was 51.2 s. The 80% rise time for the sympathetic step response or the 80% fall time for the vagal step response was estimated as the time at which the step response reached 80% of the

Table 1. *Physical characteristics*

	Sedentary	Exercise Trained
Body weight, g	642 ± 33	534 ± 33*
Ventricular weight, g	1.22 ± 0.03	1.17 ± 0.04*
Ventricular weight/body weight, g/kg	1.9 ± 0.1	2.2 ± 0.1*
Lung weight, g	2.13 ± 0.27	1.89 ± 0.38
Lung weight/body weight, g/kg	3.3 ± 0.3	3.5 ± 0.7
Performance test, s	1150 ± 165	1790 ± 389*

Values are means ± SD. *$P < 0.05$ compared with sedentary group.

steady-state response calculated by averaging the last 10 s of data of the step response.

Statistical Analysis

All data are represented as means ± SD. Data were analyzed using unpaired Student's *t*-tests (sedentary vs. exercise trained) or two-way, repeated-measures ANOVA. Values of $P < 0.05$ were considered to be significant.

RESULTS

Physical Characteristic

Morphometric characteristics and exercise capacity for sedentary and exercised-trained rats are presented in Table 1. The mean body weight of the exercised-trained rats was significantly smaller than that of the sedentary rats. The mean ventricular weight of the exercised-trained rats was slightly but significantly smaller than that of the sedentary rats. Consequently, the ventricular weight normalized by body weight was significantly greater in the exercised-trained compared with the sedentary group. The lung weight-to-body weight ratio was not different between the groups. Exercise capacity was 64% greater in the exercised-trained than in the sedentary group. The reproducibility of measuring the maximal exercise capacity was reasonably high ($y = 1.2x - 226.1$, $R^2 = 0.79$; x and y represent the first and second measurements).

Spectral Analysis of HRV and Autonomic Tone in the Conscious Resting State

The power spectral densities of R-R interval are shown in Table 2. The percentage of LF power was significantly smaller, and the percentage of HF power was significantly greater in the exercised-trained rats than in the sedentary rats. The LF/HF ratio in the exercised-trained rats was significantly smaller compared with that in the sedentary rats. HR at rest was significantly lower in the exercised-trained compared with the sedentary group (Fig. 1*A*). The intrinsic HR was similar between the groups (Fig. 1*A*). Although the sympathetic tonus was comparable between the groups, the vagal tonus tended to be greater ($P = 0.08$) in the exercised-trained compared with the sedentary group (Fig. 1*B*).

Dynamic Sympathetic and Vagal Transfer Functions

Table 3 summarizes hemodynamics during dynamic sympathetic stimulation. Sympathetic stimulation significantly increased mean HR in both sedentary and exercised-trained groups. Mean HR and AP did not differ between the groups, before and during sympathetic stimulation. Figure 2*A* illustrates the dynamic transfer function characterizing sympathetic HR control. The frequency band effect was significant ($P < 0.0001$) but the group effect was insignificant ($P = 0.5461$) in the dynamic gain values of the sympathetic transfer function by two-way, repeated-measures ANOVA. The parameters of the sympathetic transfer function were comparable between the groups (Table 4). Figure 2*B* shows the calculated step response of HR to sympathetic stimulation. The steady-state response and the 80% rise time did not differ significantly between the groups (Table 4).

Table 5 summarizes hemodynamics during dynamic vagal stimulation. Vagal stimulation significantly decreased mean HR in both sedentary and exercised-trained groups. Mean HR and AP did not differ between the groups, before and during vagal stimulation. Figure 3*A* illustrates the dynamic transfer function characterizing vagal HR control. The frequency band effect ($P < 0.0001$) and the group effect ($P < 0.0001$) were both significant in the dynamic gain values of the vagal transfer function by two-way, repeated-measures ANOVA. The estimated dynamic gain (*see* APPENDIX) tended to be greater in the exercised-trained compared with the sedentary group ($P = 0.06$, Table 6). Other parameters did not differ between the groups. Figure 3*B* shows the calculated step response of HR to vagal stimulation. The calculated steady-state response in the exercised-trained rats also tended to be greater than that in the sedentary rats ($P = 0.06$, Table 6). There was no significant difference in the 80% fall time between the groups.

Dynamic Gain Values of Sympathetic and Vagal Transfer Function Corresponding to HRV Frequency Bands

When dynamic gain values of the sympathetic transfer function were averaged for the VLF and LF (up to 0.5 Hz, see METHODS) bands, the frequency band effect was significant, but the group effect was insignificant by two-way, repeated-measures ANOVA (Fig. 4*A*). When dynamic gain values of the vagal transfer function were averaged for the VLF, LF, and HF (up to 1 Hz, see METHODS) bands, the frequency band effect was insignificant but the group effect was significant such that the dynamic gain was significantly greater in the exercised-trained compared with the sedentary group (Fig. 4*B*).

Static Sympathetic and Vagal Transfer Function

The increase in HR with stepwise sympathetic stimulation was similar between groups (Fig. 5*A*). The stimulation frequency effect was significant, while the group effect was insignificant by two-way, repeated-measures ANOVA. In contrast, the decrease in HR with stepwise vagal stimulation was greater in the exercised-trained compared with sedentary rats (Fig. 5*B*). Both the stimulation frequency effect and the group effect were significant.

Table 2. *Spectral parameters of R-R interval*

	Sedentary	Exercise Trained
Variance, ms^2	87 ± 39	90 ± 32
VLF, ms^2	73 ± 30	80 ± 30
LF, ms^2	6.3 ± 3.4	3.1 ± 3.0
LF, %	49 ± 11	36 ± 7*
HF, ms^2	8.0 ± 7.6	6.2 ± 7.1
HF, %	51 ± 11	64 ± 7*
LF/HF ratio	1.0 ± 0.5	0.6 ± 0.2*

Values are means ± SD. LF, low frequency; VLF, very low frequency; HF, high frequency; *$P < 0.05$ compared with sedentary group.

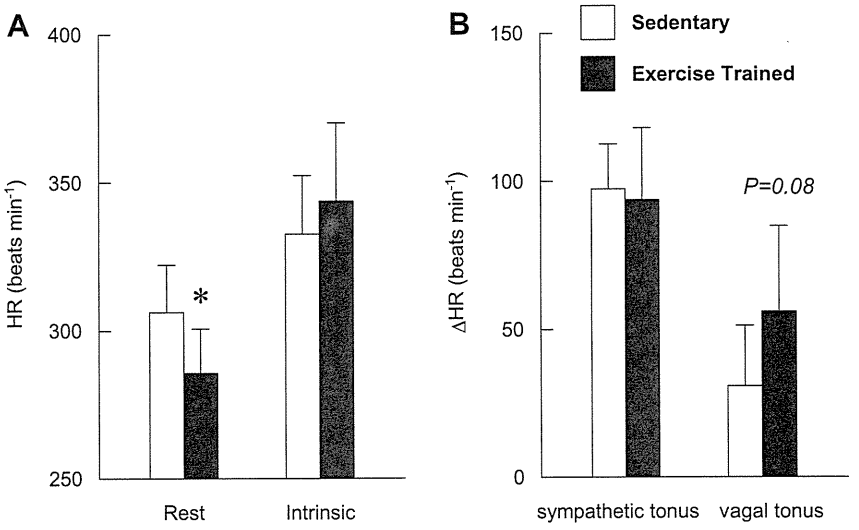

Fig. 1. Heart rate (HR) at rest and intrinsic HR (*A*) and HR sympathetic and vagal tone (*B*) obtained in sedentary and exercised-trained rats. *$P < 0.05$ compared with sedentary group.

DISCUSSION

We have examined the dynamic transfer function of autonomic HR control by using random binary sympathetic and vagal nerve stimulation in sedentary and exercised-trained rats. The major findings in the present study are *1*) that the exercise training did not alter the sympathetic transfer function substantially but augmented the dynamic gain of the vagal transfer function; and *2*) in the frequency domain, exercise training increased the dynamic HR response to vagal stimulation but not sympathetic stimulation, regardless of the frequency band. These findings are the first quantitative data on the effect of exercise training on the dynamic characteristics of peripheral HR control by the sympathetic and vagal systems.

Validity of Exercise Training

The relative ventricular hypertrophy and higher exercise capacity in the exercised-trained compared with the sedentary group suggested that exercise program used in the present study was sufficient to induce physiological adaptations commensurate with an effective training stimulus. As is well known, exercise training induces bradycardia at rest (Fig. 1*A*). Moreover, changes in the spectral parameters for R-R interval (Table 2) and autonomic tone (Fig. 1*B*) induced by the exercise training are consistent with earlier studies in rats (30, 31).

Effect of Exercise Training on Sympathetic and Vagal Transfer Function

Exercise training altered neither dynamic (Fig. 2) nor static sympathetic transfer function (Fig. 5*A*). These results are different than those reported in a previous study in which swim training significantly reduced the HR response to sympathetic nerve stimulation in a double atrial/right stellate ganglion preparation in guinea pigs (22). The discrepancy between investigations may have arisen from differences in the nerves experimentally stimulated (cervical sympathetic nerve vs. stellate ganglion), animal species studied (rats vs. guinea pigs), and/or experimental preparation utilized (in vivo vs. ex vivo). The mechanisms underlying the sympathetically mediated exercise training effect on HR are also controversial. For instance, chronotropic responsiveness to isoproterenol has been reported to be decreased in one study (15) but unchanged in another (22) by exercise training. Furthermore, in response to exercise training, the density and affinity of β-adrenoceptors in the heart have been shown to be reduced in some reports (26, 33), while unchanged in others (3, 34, 35).

Table 3. *Arterial pressure(AP) and heart rate (HR) during dynamic sympathetic stimulation protocol*

	Sedentary		Exercise Trained	
	Prestimulation	During Stimulation	Prestimulation	During Stimulation
AP, mmHg	74 ± 16	68 ± 15†	89 ± 17	84 ± 24
HR, beats/min	377 ± 25	444 ± 23†	381 ± 16	444 ± 26†

Values are means ± SD. †$P < 0.05$ compared with prestimulation.

Exercise training augmented the dynamic gain of the vagal transfer function (Fig. 2). The effect of exercise training was also significant for static vagal transfer function (Fig. 5*B*). These results are in agreement with previous studies showing that exercise training significantly augmented the HR response to vagal nerve stimulation in a double atrial/right vagal nerve preparation using mice (9, 10). In contrast, Negrao et al. (25) demonstrated that the HR response to vagal stimulation was depressed in exercised-trained rats. A possible explanation for this disparate result is that the arterial baroreflexes remained intact in the experimental preparation used in the study (25). In contrast, sinoaortic barodenervation was performed in the present investigation to minimize baroreflex-mediated changes in sympathetic efferent nerve activity. Exercise training has been shown to attenuate the baroreflex-mediated sympathetic nerve response to hypotension (11). Although speculative, in the study by Negrao et al. (25), baroreflex-mediated sympathetic activation in response to vagally-induced hypotension might have been less in exercised-trained compared with sedentary rats. Consequently, the gain of vagal stimulation might have been attenuated in exercised-trained animals relative to sedentary rats. This suggestion is reasonable given that accentuated antagonism is indicative of a diminution in background sym-

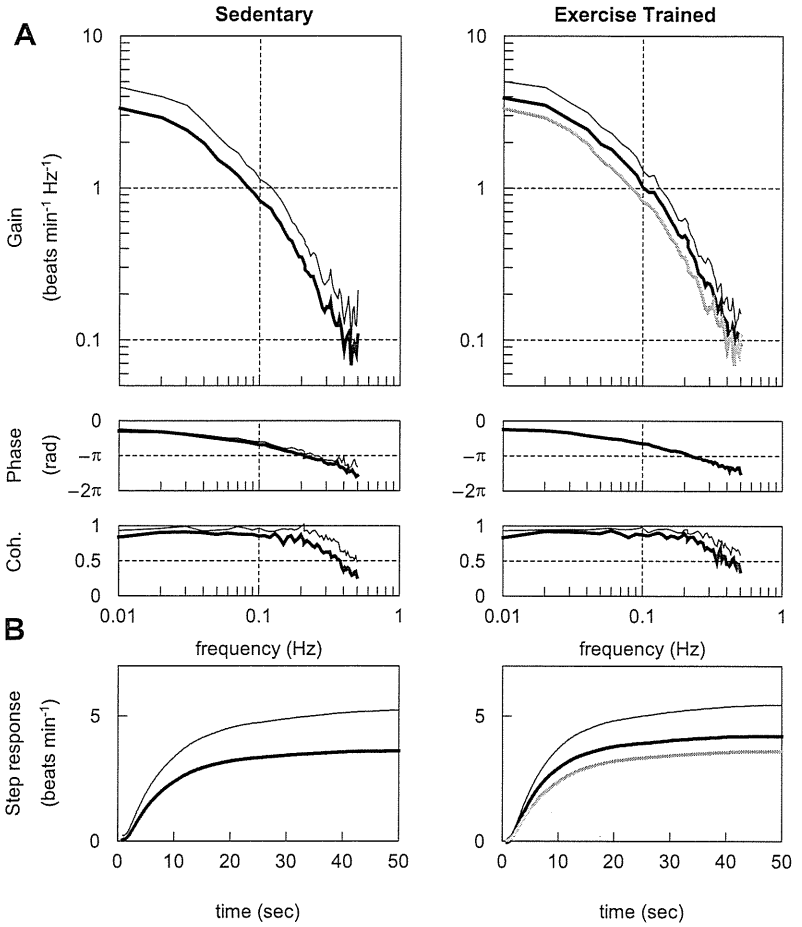

Fig. 2. *A*: transfer function from sympathetic stimulation to the HR response obtained in sedentary and exercised-trained rats. Gains (*top*), phase shifts (*middle*), and coherence (Coh.) functions (*bottom*) are presented. *B*: calculated step response to 1-Hz tonic sympathetic stimulation. Thick lines represent the mean, whereas thin lines indicate ± SD values. The gray solid curves in the gain and step response panels (*right*) duplicates the means (*left*).

pathetic tonus, which can decrease the gain of the vagal transfer function (17).

It has been documented that the intensity of exercise as well as the duration of exercise training are related to the autonomic adaptation to exercise training (28). These factors have been shown to be largely variable among different studies. A well-controlled experimental setup is needed to clarify these issues.

Dynamic Gain Values of Sympathetic and Vagal Transfer Functions Corresponding to HRV Frequency Bands

HRV is considered to reflect autonomic tone (19). The VLF component is likely to reflect changes in vasomotor tone in relation to thermoregulation and local adjustment of resistance in individual vascular beds; the LF component is considered to be a marker of sympathetic activity, although it remains a matter of debate; and the HF component mainly originates from respiratory activity and is considered to be mediated by vagal input (27). In rats, Cerutti et al. (8) determined that the LF component ranged between 0.27 and 0.74 Hz, and the HF component was > 0.75 Hz.

Averaged dynamic gain values of sympathetic transfer function for VLF and LF bands did not differ between the sedentary and exercised-trained groups (Fig. 4*A*). These results suggest that changes in the peripheral sympathetic control of HR likely do not contribute significantly to training-induced alterations in HRV. Therefore, the lower percentage of LF power and LF/HF ratio in the exercised-trained group (Table 2) may indicate reduced activation of sympathetic outflow from autonomic centers (23). In contrast, averaged dynamic gain values of vagal transfer function for VLF, LF, and HF bands (Fig. 4*B*) as

Table 4. *Sympathetic transfer function parameters and step response*

	Sedentary	Exercise Trained
Gain, beats·min^{-1}·Hz^{-1}	4.2 ± 1.5	4.5 ± 1.5
Natural frequency, Hz	0.07 ± 0.01	0.08 ± 0.01
Damping ratio	1.96 ± 0.55	1.69 ± 0.15
Lag time, s	0.71 ± 0.10	0.62 ± 0.11
Steady-state response, beats/min	3.6 ± 1.6	4.2 ± 1.2
80% rise time, s	12.9 ± 2.7	12.1 ± 3.0

Values are means ± SD. See APPENDIX for transfer function parameters.

Table 5. *AP and HR during dynamic vagal stimulation protocol*

	Sedentary		Exercise Trained	
	Prestimulation	During stimulation	Prestimulation	During stimulation
AP, mmHg	72 ± 21	68 ± 15	92 ± 14	80 ± 21
HR, beats/min	373 ± 18	327 ± 38 †	372 ± 14	301 ± 32 †

Values are means ± SD. †$P < 0.05$ compared with prestimulation.

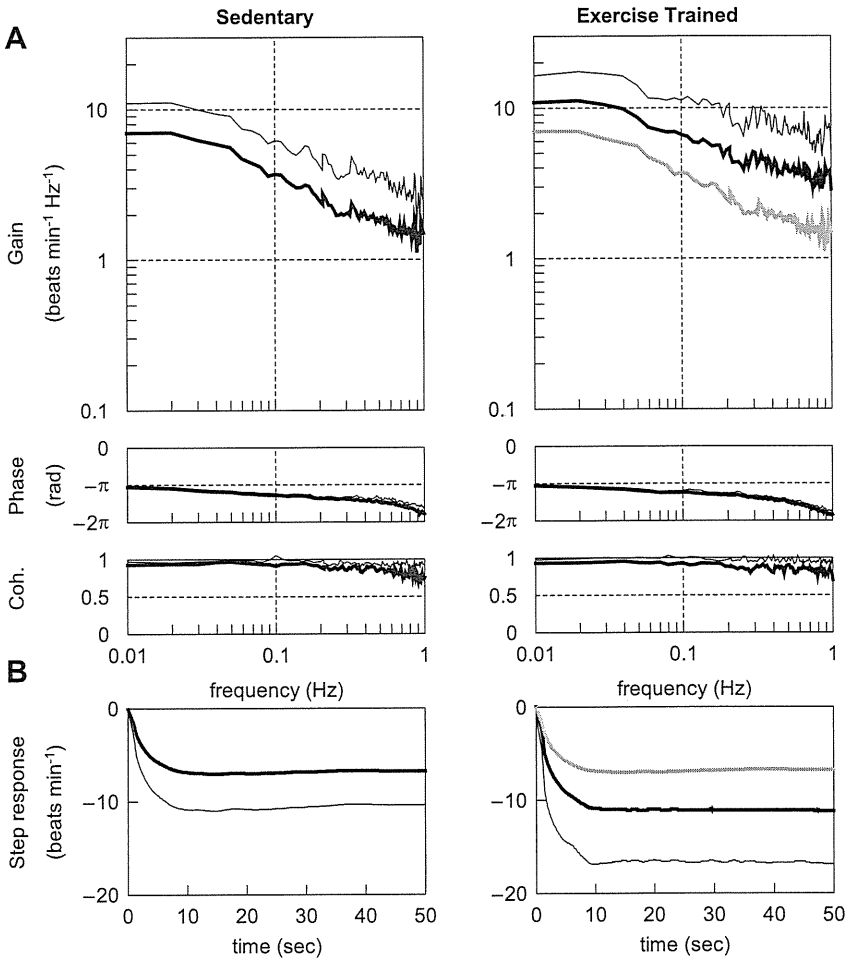

Fig. 3. *A*: transfer function from vagal stimulation to the HR response obtained in sedentary and exercised-trained rats. Gains (*top*), phase shifts (*middle*), and coherence functions (*bottom*) are presented. *B*: calculated step response to 1-Hz tonic vagal stimulation. Thick lines represent the mean, whereas thin lines indicate ± SD values. The gray solid curves in the gain and step response panels (*right*) duplicate the means (*left*).

well as the percentage of HF power (Table 2) were significantly greater in the exercised-trained compared with the sedentary group. These results suggest that the augmentation in HRV induced by exercise training is, at least in part, mediated by augmentations in the peripheral vagal control of HR.

What are the possible mechanisms underlying augmentations in the peripheral vagal control of HR? Danson and Paterson (10) have presented evidence that neuronal nitric oxide synthase may be a key enzymatic protein underlying such training-induced increases in cardiac vagal function. This group has also demonstrated that HR changes in response to vagal stimulation are enhanced by exercise training in wild-type mice but not in heterozygous neuronal nitric oxide synthase knockout mice (9). Another candidate for augmentations in the peripheral vagal control of HR is muscarinic receptors, which play a fundamental role in HR control via vagally mediated regulation. However, the effects of exercise training have been inconsistent among studies, showing both increases (12) and no change (2, 3) in muscarinic receptors in the myocardium of rats. The possibility cannot be dismissed that training-induced changes in the activity of afferent inputs mediating vagal outflow may also contribute to the alterations in HRV (4). Further investigation is needed to clarify these issues.

Table 6. *Vagal transfer function parameters and step response*

	Sedentary	Exercise Trained
Gain, beats·min^{-1}·Hz^{-1}	6.1 ± 3.0	9.7 ± 5.1#
Corner frequency, Hz	0.11 ± 0.05	0.17 ± 0.09
Lag time, s	0.10 ± 0.08	0.17 ± 0.08
Steady-state response, beats/min	−6.7 ± 3.6	−11.2 ± 5.7#
80% Fall time, s	4.3 ± 2.2	4.3 ± 1.5

Values are means ± SD. #P = 0.06 compared with sedentary group. See APPENDIX for transfer function parameters.

Perspectives and Significance

To date, the mechanisms underlying increased HRV after exercise training remain to be elucidated. HRV may reflect both the autonomic outflow from the central nervous system and the peripheral autonomic regulation of atrial pacemaker cells. In human studies, it is difficult to separately examine each factor. The findings of the present study suggest that the augmentation in HRV induced by exercise training is, at least in part, mediated by augmentations in the peripheral vagal control of HR. In other words, even if vagal outflow from the central nervous system remains unchanged after exercise training, HRV could be increased by an enhanced responsiveness in the peripheral vagal, but not sympathetic, regulation of HR.

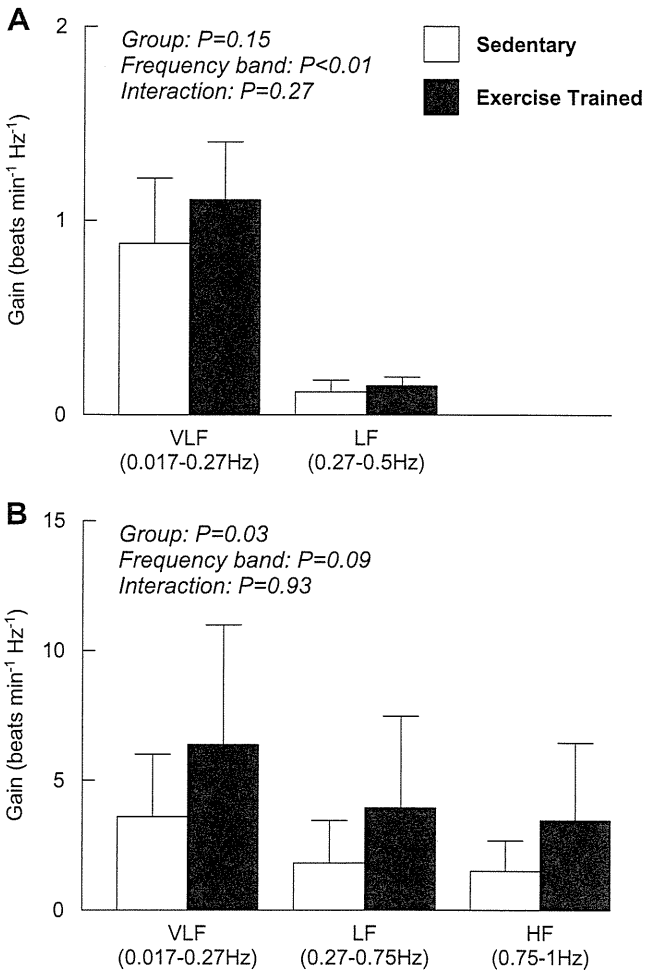

Fig. 4. Averaged sympathetic (*A*) and vagal (*B*) gain calculated from corresponding transfer function in very low frequency (VLF), low frequency (LF), and high frequency (HF) bands.

It has been well documented that decreased HRV is observed in heart failure (18) as well as in a variety of lifestyle-related diseases such as diabetes (16), hypertension (24), and obesity (1). Furthermore, reductions in HRV are related to increases in mortality rates as well as the occurrence of adverse cardiac events (32). Exercise training-induced augmentations in HRV maintain the potential to partially correct or normalize the autonomic dysfunction manifest in these disease states (4). Understanding the mechanisms contributing to the alterations in HRV induced by exercise training may significantly impact the development of novel therapeutic strategies for the treatment of autonomic dysfunction.

Limitations

There are several limitations to this study. First, the rats were slightly hyperventilated throughout the stimulation protocol. We cannot rule out the possibility that the hyperventilation might have affected the results reported. Second, dynamic sympathetic stimulation lowered mean AP in sedentary rats although sinoaortic barodenervation was performed. This may be explained by a possible difference in left ventricular functional capacity. For example, under conditions of equivalent HR, changes in systolic blood pressure were smaller in sedentary rats compared with exercised-trained rats (13). Third, the stimulation amplitude was fixed at 10 V for both sympathetic and vagal nerve stimulation. It should be noted, however, that our preliminary results indicated that 10 V was sufficiently large enough to evoke maximal HR responses. Fourth, transfer function data were obtained from anesthetized animals. This must be taken into account when interpreting the present results as anesthesia may affect the peripheral autonomic regulation of atrial pacemaker cells. Finally, we stimulated the sympathetic and vagal nerves according to a binary white noise signal. Although this method of stimulation is quite different from the physiological pattern of neuronal discharge, the coherence was near unity over the frequency range of interest. This finding indicates that the system properties do not vary considerably in response to different patterns of stimulation.

Conclusion

In the present study, it was demonstrated for the first time that exercise training did not alter dynamic sympathetic control of HR, while it did augment dynamic vagal control of HR. In addition, the group effect was significant with regard to the dynamic gain values for the vagal transfer functions corresponding to VLF, LF, and HF bands. This finding suggests that enhancements in the peripheral vagal control of HR may, at

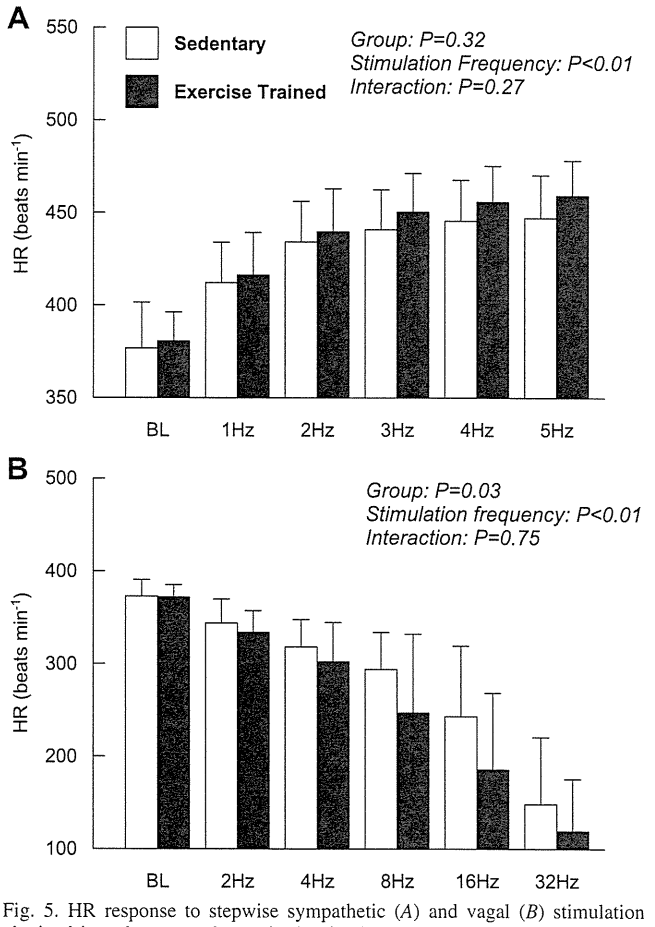

Fig. 5. HR response to stepwise sympathetic (*A*) and vagal (*B*) stimulation obtained in sedentary and exercised-trained rats.

least in part, contribute to the exercise-induced augmentation in HRV in healthy rats.

APPENDIX: TRANSFER FUNCTION ANALYSIS

The dynamic transfer function from binary white noise stimulation to the HR response was estimated based on the following procedure. Input-output data pairs of the stimulation frequency and HR were resampled at 10 Hz to be consistent with our previous study (21). Subsequently, data pairs were partitioned into eight 50% overlapping segments consisting of 1,024 data points each. For each segment, the linear trend was subtracted and a Hanning window was applied. A fast Fourier transform was then performed to obtain the frequency spectra of nerve stimulation [$N(f)$] and HR [$HR(f)$]. Over the eight segments, the power of the nerve stimulation [$S_{N\cdot N}(f)$], the power of the HR [$S_{HR\cdot HR}(f)$], and the cross-power between these two signals [$S_{N\cdot HR}(f)$] were ensemble averaged. Finally, the transfer function [$H(f)$] from nerve stimulation to the HR response was determined using the following equation (20).

$$H(f) = \frac{S_{N\text{-}HR}(f)}{S_{N\cdot N}(f)}$$

To quantify the linear dependence of the HR response on vagal or sympathetic stimulation, the magnitude-squared coherence function [Coh(f)] was estimated employing the following equation (20).

$$\mathrm{Coh}(f) = \frac{|S_{\mathrm{N\text{-}HR}}(f)|^2}{S_{\mathrm{N\cdot N}}(f) \cdot S_{\mathrm{HR\cdot HR}}(f)}$$

Coherence values range from zero to unity. Unity coherence indicates perfect linear dependence between the input and output signals; in contrast, zero coherence indicates total independence between the two signals.

Since the transfer function from sympathetic stimulation to HR response in rats approximated a second order low-pass filter with pure delay (21), we determined the parameters of the sympathetic transfer function using the following equation.

$$H(f) = \frac{K}{1 + 2\zeta\frac{f}{f_N}j + \left(\frac{f}{f_N}j\right)^2} e^{-2\pi f j L}$$

where K is dynamic gain (in beats·min^{-1}·Hz^{-1}), f_N is the natural frequency (in Hz), ζ is the damping ratio, L is lag time (in s), and f and j represent frequency and imaginary units, respectively. These parameters were estimated by means of an iterative nonlinear least squares regression.

Since the transfer function from vagal stimulation to HR response in rats approximated a first-order, low-pass filter with pure delay (21), we determined the parameters of the vagal transfer function using the following equation.

$$H(f) = \frac{-K}{1 + \frac{f}{f_C}j} e^{-2\pi f j L}$$

where K represents the dynamic gain (in beats·min^{-1}·Hz^{-1}), fc denotes the corner frequency (in Hz), L denotes the lag time (in s), and f and j represent frequency and imaginary units, respectively. The negative sign in the numerator indicates the negative HR response to vagal stimulation. These parameters were estimated by means of an iterative nonlinear least squares regression.

GRANTS

This study was supported by Health and Labor Sciences Research Grants H18-nano-Ippan-003, H19-nano-Ippan-009, H20-katsudo-Shitei-007, and H21-nano-Ippan-005 from the Ministry of Health, Labor and Welfare of Japan, by Grants-in-Aid for Scientific Research No. 19700559 from the Ministry of Education, Culture, Sports, Science and Technology in Japan, and by the Industrial Technology Research Grant Program from New Energy and Industrial Technology Development Organization of Japan. M. Mizuno was supported from Research Fellowships of the Japan Society for the Promotion of Science for Young Scientists.

DISCLOSURES

No conflicts of interest, financial or otherwise, are declared by the author(s).

REFERENCES

1. **Arone LJ, Mackintosh R, Rosenbaum M, Leibel RL, Hirsch J.** Autonomic nervous system activity in weight gain and weight loss. *Am J Physiol Regul Integr Comp Physiol* 269: R222–R225, 1995.
2. **Barbier J, Rannou-Bekono F, Marchais J, Berthon PM, Delamarche P, Carre F.** Effect of training on β1-, β2-, β3-adrenergic and M2 muscarinic receptors in rat heart. *Med Sci Sports Exerc* 36: 949–954, 2004.
3. **Barbier J, Reland S, Ville N, Rannou-Bekono F, Wong S, Carre F.** The effects of exercise training on myocardial adrenergic and muscarinic receptors. *Clin Auton Res* 16: 61–65, 2006.
4. **Billman GE.** Cardiac autonomic neural remodeling and susceptibility to sudden cardiac death: effect of endurance exercise training. *Am J Physiol Heart Circ Physiol* 297: H1171–H1193, 2009.
5. **Blomqvist CG, Saltin B.** Cardiovascular adaptations to physical training. *Annu Rev Physiol* 45: 169–189, 1983.
6. **Brenner DA, Apstein CS, Saupe KW.** Exercise training attenuates age-associated diastolic dysfunction in rats. *Circulation* 104: 221–226, 2001.
7. **Buch AN, Coote JH, Townend JN.** Mortality, cardiac vagal control and physical training–what's the link? *Exp Physiol* 87: 423–435, 2002.
8. **Cerutti C, Gustin MP, Paultre CZ, Lo M, Julien C, Vincent M, Sassard J.** Autonomic nervous system and cardiovascular variability in rats: a spectral analysis approach. *Am J Physiol Heart Circ Physiol* 261: H1292–H1299, 1991.
9. **Danson EJ, Mankia KS, Golding S, Dawson T, Everatt L, Cai S, Channon KM, Paterson DJ.** Impaired regulation of neuronal nitric oxide synthase and heart rate during exercise in mice lacking one nNOS allele. *J Physiol* 558: 963–974, 2004.
10. **Danson EJ, Paterson DJ.** Enhanced neuronal nitric oxide synthase expression is central to cardiac vagal phenotype in exercise-trained mice. *J Physiol* 546: 225–232, 2003.
11. **DiCarlo SE, Bishop VS.** Exercise training attenuates baroreflex regulation of nerve activity in rabbits. *Am J Physiol Heart Circ Physiol* 255: H974–H979, 1988.
12. **Favret F, Henderson KK, Clancy RL, Richalet JP, Gonzalez NC.** Exercise training alters the effect of chronic hypoxia on myocardial adrenergic and muscarinic receptor number. *J Appl Physiol* 91: 1283–1288, 2001.
13. **Fitzsimons DP, Bodell PW, Herrick RE, Baldwin KM.** Left ventricular functional capacity in the endurance-trained rodent. *J Appl Physiol* 69: 305–312, 1990.
14. **Goldsmith RL, Bigger JT Jr, Steinman RC, Fleiss JL.** Comparison of 24-hour parasympathetic activity in endurance-trained and untrained young men. *J Am Coll Cardiol* 20: 552–558, 1992.
15. **Hammond HK, White FC, Brunton LL, Longhurst JC.** Association of decreased myocardial β-receptors and chronotropic response to isoproterenol and exercise in pigs following chronic dynamic exercise. *Circ Res* 60: 720–726, 1987.
16. **Ikeda T, Matsubara T, Sato Y, Sakamoto N.** Circadian blood pressure variation in diabetic patients with autonomic neuropathy. *J Hypertens* 11: 581–587, 1993.
17. **Kawada T, Ikeda Y, Sugimachi M, Shishido T, Kawaguchi O, Yamazaki T, Alexander J Jr, Sunagawa K.** Bidirectional augmentation of heart rate regulation by autonomic nervous system in rabbits. *Am J Physiol Heart Circ Physiol* 271: H288–H295, 1996.
18. **La Rovere MT, Pinna GD, Maestri R, Mortara A, Capomolla S, Febo O, Ferrari R, Franchini M, Gnemmi M, Opasich C, Riccardi PG, Traversi E, Cobelli F.** Short-term heart rate variability strongly predicts sudden cardiac death in chronic heart failure patients. *Circulation* 107: 565–570, 2003.

19. **Malliani A, Pagani M, Lombardi F, Cerutti S.** Cardiovascular neural regulation explored in the frequency domain. *Circulation* 84: 482–492, 1991.
20. **Marmarelis P, Marmarelis V.** The white noise method in system identification. In: *Analysis of Physiological Systems*. New York: Plenum, 1978, p. 131–221.
21. **Mizuno M, Kawada T, Kamiya A, Miyamoto T, Shimizu S, Shishido T, Smith SA, Sugimachi M.** Dynamic characteristics of heart rate control by the autonomic nervous system in rats. *Exp Physiol* 95: 919–925, 2010.
22. **Mohan RM, Choate JK, Golding S, Herring N, Casadei B, Paterson DJ.** Peripheral pre-synaptic pathway reduces the heart rate response to sympathetic activation following exercise training: role of NO. *Cardiovasc Res* 47: 90–98, 2000.
23. **Mueller PJ.** Exercise training attenuates increases in lumbar sympathetic nerve activity produced by stimulation of the rostral ventrolateral medulla. *J Appl Physiol* 102: 803–813, 2007.
24. **Mussalo H, Vanninen E, Ikaheimo R, Laitinen T, Laakso M, Lansimies E, Hartikainen J.** Heart rate variability and its determinants in patients with severe or mild essential hypertension. *Clin Physiol* 21: 594–604, 2001.
25. **Negrao CE, Moreira ED, Santos MC, Farah VM, Krieger EM.** Vagal function impairment after exercise training. *J Appl Physiol* 72: 1749–1753, 1992.
26. **Nieto JL, Laviada ID, Guillen A, Haro A.** Adenylyl cyclase system is affected differently by endurance physical training in heart and adipose tissue. *Biochem Pharmacol* 51: 1321–1329, 1996.
27. **Pagani M, Lombardi F, Guzzetti S, Rimoldi O, Furlan R, Pizzinelli P, Sandrone G, Malfatto G, Dell'Orto S, Piccaluga E.** Power spectral analysis of heart rate and arterial pressure variabilities as a marker of sympatho-vagal interaction in man and conscious dog. *Circ Res* 59: 178–193, 1986.
28. **Sandercock GR, Bromley PD, Brodie DA.** Effects of exercise on heart rate variability: inferences from meta-analysis. *Med Sci Sports Exerc* 37: 433–439, 2005.
29. **Schwarz P, Diem R, Dun NJ, Forstermann U.** Endogenous and exogenous nitric oxide inhibits norepinephrine release from rat heart sympathetic nerves. *Circ Res* 77: 841–848, 1995.
30. **Souza SB, Flues K, Paulini J, Mostarda C, Rodrigues B, Souza LE, Irigoyen MC, De Angelis K.** Role of exercise training in cardiovascular autonomic dysfunction and mortality in diabetic ovariectomized rats. *Hypertension* 50: 786–791, 2007.
31. **Tezini GC, Silveira LC, Villa-Cle PG Jr, Jacinto CP, Di Sacco TH, Souza HC.** The effect of aerobic physical training on cardiac autonomic control of rats submitted to ovariectomy. *Menopause* 16: 110–116, 2009.
32. **Tsuji H, Larson MG, Venditti FJ Jr, Manders ES, Evans JC, Feldman CL, Levy D.** Impact of reduced heart rate variability on risk for cardiac events. The Framingham Heart Study. *Circulation* 94: 2850–2855, 1996.
33. **Werle EO, Strobel G, Weicker H.** Decrease in rat cardiac β1- and β2-adrenoceptors by training and endurance exercise. *Life Sci* 46: 9–17, 1990.
34. **Williams RS.** Physical conditioning and membrane receptors for cardioregulatory hormones. *Cardiovasc Res* 14: 177–182, 1980.
35. **Williams RS, Schaible TF, Bishop T, Morey M.** Effects of endurance training on cholinergic and adrenergic receptors of rat heart. *J Mol Cell Cardiol* 16: 395–403, 1984.
36. **Yamamoto K, Miyachi M, Saitoh T, Yoshioka A, Onodera S.** Effects of endurance training on resting and post-exercise cardiac autonomic control. *Med Sci Sports Exerc* 33: 1496–1502, 2001.

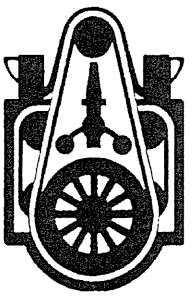

Electrocardiographic Characteristics and *SCN5A* Mutations in Idiopathic Ventricular Fibrillation Associated With Early Repolarization

Hiroshi Watanabe, MD, PhD, FESC; Akihiko Nogami, MD, PhD; Kimie Ohkubo, MD, PhD; Hiro Kawata, MD, PhD; Yuka Hayashi, MD; Taisuke Ishikawa, DVM; Takeru Makiyama, MD, PhD; Satomi Nagao, MD; Nobue Yagihara, MD; Naofumi Takehara, MD, PhD; Yuichiro Kawamura, MD, PhD; Akinori Sato, MD, PhD; Kazuki Okamura, MD, PhD; Yukio Hosaka, MD, PhD; Masahito Sato, MD, PhD; Satoki Fukae, MD, PhD; Masaomi Chinushi, MD, PhD; Hirotaka Oda, MD, PhD; Masaaki Okabe, MD, PhD; Akinori Kimura, MD, PhD; Koji Maemura, MD, PhD; Ichiro Watanabe, MD, PhD, FHRS; Shiro Kamakura, MD, PhD; Minoru Horie, MD, PhD; Yoshifusa Aizawa, MD, PhD; Wataru Shimizu, MD, PhD; Naomasa Makita, MD, PhD

Background—Recently, we and others reported that early repolarization (J wave) is associated with idiopathic ventricular fibrillation. However, its clinical and genetic characteristics are unclear.

Methods and Results—This study included 50 patients (44 men; age, 45±17 years) with idiopathic ventricular fibrillation associated with early repolarization, and 250 age- and sex-matched healthy controls. All of the patients had experienced arrhythmia events, and 8 (16%) had a family history of sudden death. Ventricular fibrillation was inducible by programmed electric stimulation in 15 of 29 patients (52%). The heart rate was slower and the PR interval and QRS duration were longer in patients with idiopathic ventricular fibrillation than in controls. We identified nonsynonymous variants in *SCN5A* (resulting in A226D, L846R, and R367H) in 3 unrelated patients. These variants occur at residues that are highly conserved across mammals. His-ventricular interval was prolonged in all of the patients carrying an *SCN5A* mutation. Sodium channel blocker challenge resulted in an augmentation of early repolarization or development of ventricular fibrillation in all of 3 patients, but none was diagnosed with Brugada syndrome. In heterologous expression studies, all of the mutant channels failed to generate any currents. Immunostaining revealed a trafficking defect in A226D channels and normal trafficking in R367H and L846R channels.

Conclusions—We found reductions in heart rate and cardiac conduction and loss-of-function mutations in *SCN5A* in patients with idiopathic ventricular fibrillation associated with early repolarization. These findings support the hypothesis that decreased sodium current enhances ventricular fibrillation susceptibility. (***Circ Arrhythm Electrophysiol.* 2011;4:874-881.**)

Key Words: arrhythmia ■ sodium channel ■ electrophysiology ■ genetics ■ mutations

Early repolarization or J-wave is characterized by an elevation at the junction between the end of the QRS complex and the beginning of the ST-segment (J-point) in a 12-lead ECG and generally has been considered benign for decades.[1] However, early repolarization can be observed under various negative biological conditions, such as low body temperature and ischemia,[2–4] and there is increasing evidence that early repolarization is associated with an increased risk of ventricular fibrillation and sudden cardiac death.[5–7]

Clinical Perspective on p 881

Received February 2, 2011; accepted October 5, 2011.

From the Division of Cardiology (H.W., Y.H., S.N., N.Y., A.S., K.O., M.C., Y.A.), Niigata University School of Medicine, Niigata; Division of Heart Rhythm Management (A.N.), Yokohama Rosai Hospital, Yokohama; Division of Cardiology (K.O., I.W.), Department of Medicine, Nihon University School of Medicine, Tokyo; Division of Arrhythmia and Electrophysiology (H.K., S.K., W.S.), Department of Cardiovascular Medicine, National Cerebral and Cardiovascular Center, Suita; Department of Molecular Pathogenesis (T.I., A.K.), Medical Research Institute, Tokyo Medical and Dental University, Tokyo; Department of Cardiovascular Medicine (T.M.), Kyoto University Graduate School of Medicine, Kyoto; Department of Internal Medicine (N.T., Y.K.), Division of Cardiovascular Respiratory and Neurology, Asahikawa Medical University, Asahikawa; Department of Cardiology (Y.H., H.O.), Niigata City General Hospital, Niigata; Cardiovascular Center (M.S., M.O.), Tachikawa General Hospital, Nagaoka; Departments of Cardiovascular Medicine (S.F., K.M.) and Molecular Physiology (N.M.), Nagasaki University Graduate School of Biomedical Sciences, Nagasaki; Department of Cardiovascular and Respiratory Medicine (M.H.), Shiga University of Medical Science, Shiga, Japan.

Correspondence to Hiroshi Watanabe, MD, PhD, FESC, Division of Cardiology, Niigata University Graduate School of Medical and Dental Sciences, 1-754 Asahimachidori, Niigata 951-8510 Japan. E-mail hiroshi7@med.niigata-u.ac.jp

Circ Arrhythm Electrophysiol **is available at http://circep.ahajournals.org** **DOI: 10.1161/CIRCEP.111.963983**

In previous studies, including our own, early repolarization in the inferior or lateral leads was associated with pathogenesis in idiopathic ventricular fibrillation.[5,6] Moreover, early repolarization in the right precordial leads also has been associated with idiopathic ventricular fibrillation.[8] Heritability of early repolarization has been shown in a recent population-based study,[9] and as in other arrhythmia syndromes such as long QT syndrome and Brugada syndrome,[10] ion channel genes are responsible for idiopathic ventricular fibrillation associated with early repolarization.[11–13] A mutation in *KCNJ8*, which encodes a pore-forming subunit of the ATP-sensitive potassium channel, has been identified in idiopathic ventricular fibrillation with early repolarization.[11,14] Mutations in L-type calcium channel genes, including *CACNA1C*, *CACNB2B*, and *CACNA2D1*, also have been associated with idiopathic ventricular fibrillation with early repolarization.[12]

In this study, we compared electrocardiographic parameters between patients with idiopathic ventricular fibrillation and healthy controls and found that heart rate and cardiac conduction were slow in patients with idiopathic ventricular fibrillation. Furthermore, we screened patients with idiopathic ventricular fibrillation for mutations in *SCN5A*, which encodes the predominant cardiac sodium channel α subunit and is critical for cardiac conduction. Here, we present the clinical and in vitro electrophysiological characteristics in idiopathic ventricular fibrillation associated with early repolarization.

Methods

Study Populations

This study included patients with idiopathic ventricular fibrillation and early repolarization who were referred to our institutions. Patients were diagnosed with idiopathic ventricular fibrillation if they had no structural heart disease as identified using echocardiography, coronary angiography, and left ventriculography. Baseline electrophysiological studies without antiarrhythmic drugs were performed based on the indication of each institution. Early repolarization was defined as an elevation of the J-point, either as QRS slurring or notching $\geq$0.1 mV $\geq$2 consecutive leads in the 12-lead ECG.[5] Patients were excluded if they had a short QT interval (corrected QT interval using Bazett formula <340 ms) or a long QT interval (corrected QT interval >440 ms) in the 12-lead ECG.[15,16] All patients received sodium channel blocker challenge, and patients with Brugada type ST-segment elevations at baseline or after sodium channel blocker challenge were excluded.[17] Twelve-lead electrocardiograms recorded in the absence of antiarrhythmic drugs were compared between patients with idiopathic ventricular fibrillation and control subjects who were matched to patients with idiopathic ventricular fibrillation based on gender and age (patient: control ratio, 1:5). Control subjects were selected from 86 068 consecutive electrocardiograms stored in the ECG database in Niigata University Medical and Dental Hospital from May 7, 2003 to July 2, 2009.[18] Control subjects who had a normal QT interval (corrected QT interval, 360 to 440 ms) and no cardiovascular disease or medication use were included. Control subjects with Brugada type ST-segment elevations or early repolarization were excluded.

Genetic Analysis

All probands and family members who participated in the study gave written informed consent before genetic and clinical investigations in accordance with the standards of the Declaration of Helsinki and local ethics committees. Genetic analysis was performed on genomic DNA extracted from peripheral white blood cells using standard methods. The coding regions of *KCNQ1*, *KCNH2*, *SCN5A*, *KCNE1*, *KCNE2*, and *KCNJ8* were amplified by PCR using exon-flanking intronic primers,[19–21] and direct DNA sequencing was performed using ABI 310, 3130, and 3730 genetic analyzers (Applied Biosystems, Foster City, CA).[22]

Generation of Expression Vectors and Transfection in Mammalian Cell Lines

Full-length human *SCN5A* cDNA was subcloned into the mammalian expression plasmid pcDNA3.1+ (Invitrogen, Carlsbad, CA).[22] Mutant constructs were prepared using a QuikChange site-directed mutagenesis kit (Stratagene, La Jolla, CA) according to the manufacturer's instructions. The human cell line tsA201 was transiently transfected with wild-type or mutant *SCN5A* plasmid using Lipofectamine LTX (Invitrogen), in combination with a bicistronic plasmid (pCD8-IRES-hβ1) encoding CD8 and the human sodium channel β1 subunit (hβ1) to visually identify cells expressing heterologous hβ1 using Dynabeads M-450 CD8 (Invitrogen).[22] Electrophysiological measurements were performed 24 to 72 hours after transfection.

Electrophysiology

Sodium currents were recorded using the whole-cell patch clamp technique as previously described.[22] Electrode resistance ranged from 0.8 to 1.5 mol/LΩ. Data were acquired using an Axopatch 200B patch clamp amplifier and pCLAMP8 software (Axon Instruments). Sodium currents were filtered at 5 kHz (−3 dB, 4-pole Bessel filter) and were digitally sampled at 50 kHz using an analog-to-digital interface (Digidata 1322A; Molecular Devices, Sunnyvale, CA). Experiments were performed at room temperature (20 to 22°C). Voltage errors were minimized using series resistance compensation (generally 80%). Cancellation of the capacitance transients and leak subtraction were performed using an online P/4 protocol. The time from establishing the whole-cell configuration to the onset of recording was consistent (5 minutes) between cells to exclude possible time-dependent shifts of steady-state inactivation. The pulse protocol cycle time was 10 s. The data were analyzed using Clampfit 10 (Molecular Devices) and SigmaPlot 9 software (Aspire Software International, Ashburn, VA). The holding potential was −120 mV. The bath solution contained the following (in mmol/L): 145 NaCl, 4 KCl, 1.8 $CaCl_2$, 1 $MgCl_2$, 10 HEPES, and 10 glucose, pH 7.35 (adjusted with NaOH). The pipette solution (intracellular solution) contained the following (in mmol/L): 10 NaF, 110 CsF, 20 CsCl, 10 EGTA, and 10 HEPES, pH 7.35 (adjusted with CsOH).

Immunocytochemistry

For immunocytochemistry, the FLAG epitope was inserted between residues 153 and 154 of the extracellular linker S1-S2 in domain I. The FLAG insertion into the S1-S2 linker previously has been shown to have no effect on channel gating or cell surface expression.[22,23] Immunocytochemistry was performed in HEK293 cells transfected with wild-type or mutant *SCN5A* plasmid as described previously.[22,24] After 48 hours of transfection, the cells were washed with phosphate-buffered saline, fixed in 4% paraformaldehyde, and permeabilized with 0.15% Triton X-100 in phosphate-buffered saline with 3% bovine serum albumin. Then the cells were stained with anti-FLAG polyclonal antibody (F7425; Sigma-Aldrich, St Louis, MO; 1:100) for 1 hour at room temperature. Protein reacting with antibody was visualized with Alexa Fluor 568–labeled secondary antibody (A-11011, Invitrogen, 1:1000). Images were collected using a Zeiss LSM 510 laser confocal microscope and analyzed using LSM 4.0 software.

Data Analysis

Differences in parameters between patients with idiopathic ventricular fibrillation and control subjects were analyzed using conditional logistic regression models. To exclude the effects of multicollinearity among electrocardiographic parameters, each electrocar-

Table 1. Electrocardiographic Parameters

	IVF Patients N=50	Controls N=250	OR (95% CI)/ 10 Unit Increase	*P* Value
Male sex, N (%)	44 (88)	220 (88)	...	...
Age, y	45±17	45±16	...	...
Heart rate, beats/min	62±9	70±14	0.62 (0.47–0.81)	<0.001
PR interval, ms	175±34	147±20	1.32 (1.22–1.43)	<0.001
QRS interval, ms	96±14	89±8	1.63 (1.31–2.02)	<0.001
QTc, ms	388±25	397±22	0.85 (0.75–0.98)	0.02

IVF indicates idiopathic ventricular fibrillation; OR, odds ratio; QTc, corrected QT interval.

diographic parameter was separately tested in the logistic models. All statistical analyses were performed with SPSS, version 12.0 (SPSS Inc, Chicago, IL). A 2-sided $P<0.05$ was considered statistically significant. Values are expressed as mean±SD. The study protocol was approved by the ethics committee of each institution.

Results

We identified 50 patients with idiopathic ventricular fibrillation and early repolarization (44 men [88%]; mean age, 45±17 years). All of the patients had experienced arrhythmia events, and 8 (16%) had a family history of sudden death.

Electrocardiographic parameters were compared between 50 patients with idiopathic ventricular fibrillation and 250 healthy control subjects without cardiovascular disease and not taking medication who were matched with gender and age (Table 1). The heart rate was slower, and the PR interval and QRS duration were longer in patients with idiopathic ventricular fibrillation compared with control subjects. The corrected QT interval was shorter in patients with idiopathic ventricular fibrillation than control subjects. No patient with idiopathic ventricular fibrillation showed type I Brugada electrocardiograms in repeated recordings.[25] Sodium channel blockers were administered in all patients, and Brugada type electrocardiograms were not provoked in any of these patients.[25] Electrophysiological study was performed in 29 patients. His-ventricular interval was 48±9 ms, and 4 patients had prolonged His-ventricular time ≥55 ms.[26] Ventricular fibrillation was inducible by programmed electric stimulation in 15 patients (52%).

We screened for mutations in *SCN5A* in 26 unrelated patients with idiopathic ventricular fibrillation and identified 3 mutations (A226D, R367H, and L846R) in 3 patients (Figure 1, Table 2). R367H and L846R are predicted to be located in the pore region. These mutations were not found in the genomes of 200 healthy control individuals. Two of the patients exhibited prolongation of the PR interval, and sodium channel blocker challenge was negative for Brugada syndrome in all of them. Alignment of the amino acid sequences from multiple species demonstrated that the amino acids substituted by mutations are highly conserved, supporting the importance of these amino acids. A226D and L846R, but not R367H, are predicted to change the electric charge of substituted amino acids.

A missense mutation, A226D (Figure 1A), was identified in a 36-year-old man (patient 1) resuscitated from ventricular fibrillation. He had experienced multiple episodes of syncope. The physical examination and echocardiography were normal. His ECG showed prolongation of the PR interval and early repolarization in leads II, III, and aVF, and J-point/ST-segment elevation in lead V1 (Figure 2A). Administration of pilsicainide augmented early repolarization in the inferior leads and induced ventricular fibrillation, but did not produce a type I Brugada ECG in the right precordial leads (Figure 2B). Electrophysiological study revealed prolongation of His-ventricular interval (68 ms), and ventricular fibrillation was induced by programmed electric stimulation. The patient's family history was negative for syncope, sudden cardiac death, and epilepsy.

A missense mutation L846R (Figure 1B) was identified in a 27-year-old man (patient 2). He was admitted after multiple episodes of syncope, and polymorphic ventricular tachycardia was documented when he lost consciousness. The physical examination and echocardiography were normal. His ECG

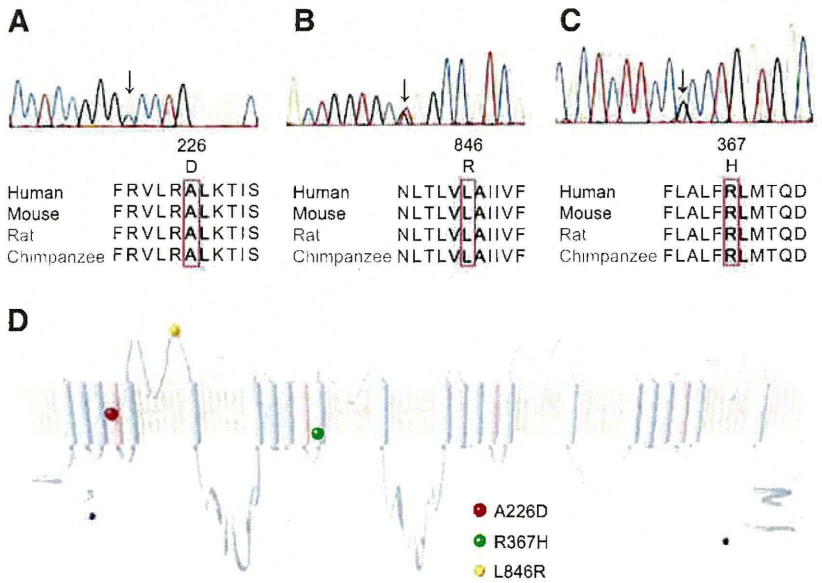

Figure 1. Mutations in *SCN5A* identified in patients with idiopathic ventricular fibrillation associated with early repolarization. **A**, The c.677C→A mutation in *SCN5A* resulting in p.A226D found in patient 1. **B**, The c.2537T→G mutation in *SCN5A*, resulting in p.L846R found in patient 2. **C**, The c.1100G→A mutation in *SCN5A*, resulting in p.R367H found in patient 3. We previously reported the R367H mutation (modified from Takehara et al[27]). **D**, Predictive topology of the SCN5A channel. Circles indicate the locations of the mutations.

Table 2. Characteristics of Idiopathic Ventricular Fibrillation Patients With *SCN5A* Mutations

Patient No.	Sex	Age at Onset (y)	Family History of SCD	Presenting Symptom	Location of J Wave	Other ECG Abnormalities	Response to Sodium Channel Blocker	Amino Acid Substitution
1	M	36	N	Aborted SCD	II, III, aVF, V1	PR prolongation	Augmentation of J-point amplitude and VF	A226D
2	M	27	Y	Aborted SCD	I, II, III, aVF	PR prolongation	Marked QRS prolongation and VF	L846R
3	F	37	N	Aborted SCD	II, III, aVF, V2	N	Augmentation of J-point amplitude and marked QRS prolongation	R367H

ECG indicates electrocardiogram; SCD, sudden cardiac death.

showed prolongation of the PR interval and early repolarization in lead III (Figure 2C). During the recovery phase of exercise testing, the amplitude of the J-point/ST-segment was augmented in leads I, II, III, and aVF, and ventricular fibrillation was induced. Pilsicainide caused marked prolongation of QRS duration and augmented the J-point/ST-segment amplitude in leads V1 and V2, followed by the development of ventricular fibrillation (Figure 2C and 2D). Pilsicainide did not produce a type I Brugada ECG. During electrophysiological study, His-ventricular interval was 55 ms. His uncle died suddenly.

We previously reported a missense mutation R367H in patient 3 as a case with Brugada syndrome (Figure 1C).[27] However, idiopathic ventricular fibrillation associated with early repolarization was diagnosed at a later time because a type 1 Brugada ECG has never been seen spontaneously or after the administration of sodium channel blocker in more than 1 right precordial lead, and thus the diagnostic criteria for Brugada syndrome were not fulfilled.[25] When the patient admitted to the hospital after recurrent episodes of syncope, early repolarization was present in the inferior and right precordial leads (Figure 2E). After sinus pause, early repolarization was augmented in leads II, III, and aVF, followed by the development of ventricular fibrillation after a few hours of the admission (Figure 2F). Procainamide further exaggerated early repolarization but did not produce a type I

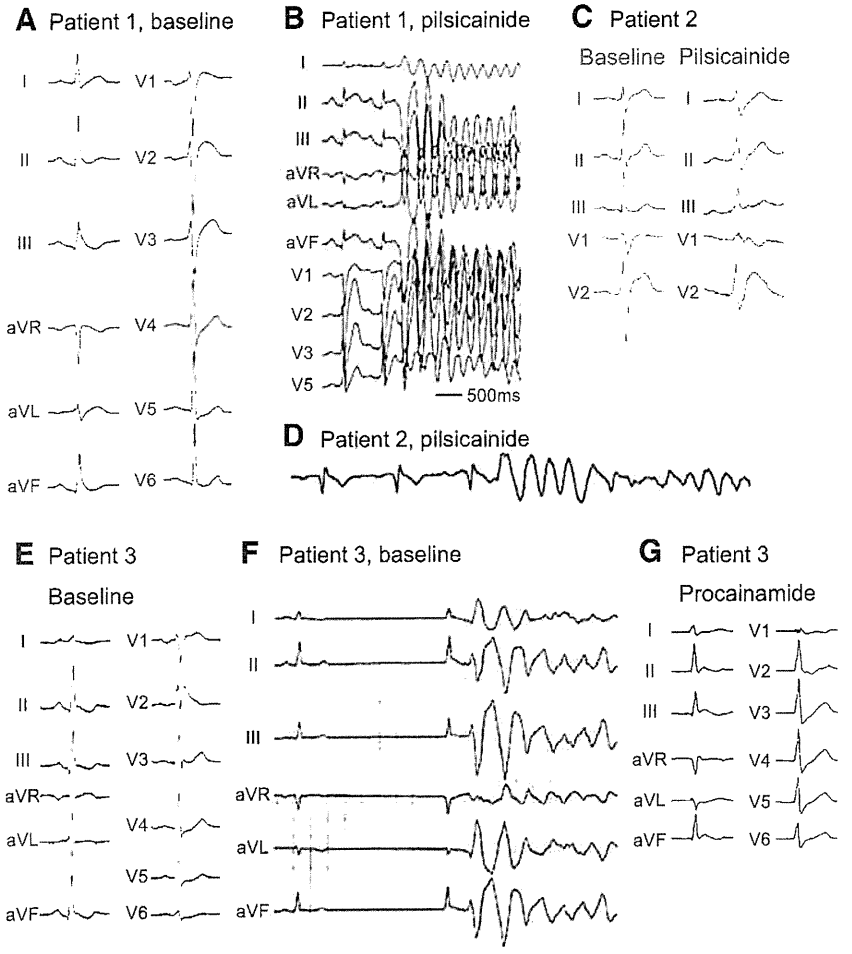

Figure 2. Electrocardiograms of patients with idiopathic ventricular fibrillation and a mutation in *SCN5A*. **A**, Early repolarization was present in the inferior and right precordial leads in patient 1. **B**, After administration of pilsicainide, early repolarization was augmented and ventricular fibrillation developed. **C** and **D**, Pilsicainide caused marked prolongation of QRS duration and J-point elevation in the right precordial leads, followed by the development of ventricular fibrillation in patient 2. **E**, Early repolarization was present in the inferior leads and right precordial leads in patient 3. **F**, The augmentation of early repolarization after sinus pause, followed by ventricular fibrillation. **G**, After the administration of procainamide, early repolarization was augmented in the inferior. In all patients, sodium channel blockers did not provoke a type I Brugada ECG. **E**, **F**, and **G** were modified from Takehara et al.[27]

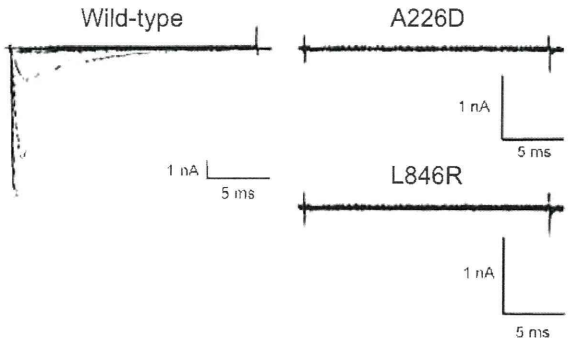

Figure 3. Electrophysiological characteristics of the *SCN5A* mutants. Representative traces of sodium current demonstrating that all of the mutant channels failed to generate any currents. We previously reported that R367H mutant fails to generate any currents.[27]

Brugada ECG (Figure 2G). During electrophysiological study, His-ventricular time was prolonged (65 ms) and ventricular fibrillation was not induced. The patient's family history was negative for syncope, sudden cardiac death, and epilepsy.

The electrophysiological characteristics of the mutant sodium channels were assessed in transfected mammalian cells using the whole-cell patch-clamp technique. Figure 3 shows representative current traces in cells expressing wild-type or mutant SCN5A channels. There was no detectable current in A226D, R367H,[27] and L846R mutant channels. Immunostaining revealed that cells expressing A226D channels showed cytoplasmic fluorescence, while cells expressing wild-type channels showed marked peripheral fluorescence, suggesting that the mutation results in trafficking defect (Figure 4). Cells expressing R367H channels and those expressing L846R channels showed a similar fluorescence pattern to wild-type channels, suggesting that these mutations do not affect trafficking.

Discussion

In this study, patients with idiopathic ventricular fibrillation associated with early repolarization exhibited slower heart rate and slower cardiac conduction properties than did controls. We found rare, nonsynonymous variants in *SCN5A* in patients who had idiopathic ventricular fibrillation associated with early repolarization. These variants affect highly conserved residues, and all of the mutant SCN5A channels failed to generate any currents when expressed in heterologous expression systems. Immunostaining experiments suggested 2 possible mechanisms for the sodium channel dysfunction by the *SCN5A* mutations, a defect of channel trafficking to cell surface in A226D and critical alterations of the structures required for the sodium ion permeation or gating in R367H and L846R that are predicted to be located at the pore region.

Loss-of-function mutations in *SCN5A* are associated with a wide range of inherited arrhythmia syndromes, including Brugada syndrome, progressive cardiac conduction disease, and sick sinus syndrome.[28–30] Furthermore, our results suggest that *SCN5A* is a causative gene of idiopathic ventricular fibrillation associated with early repolarization. Evidence supporting disease causality of the mutations includes the

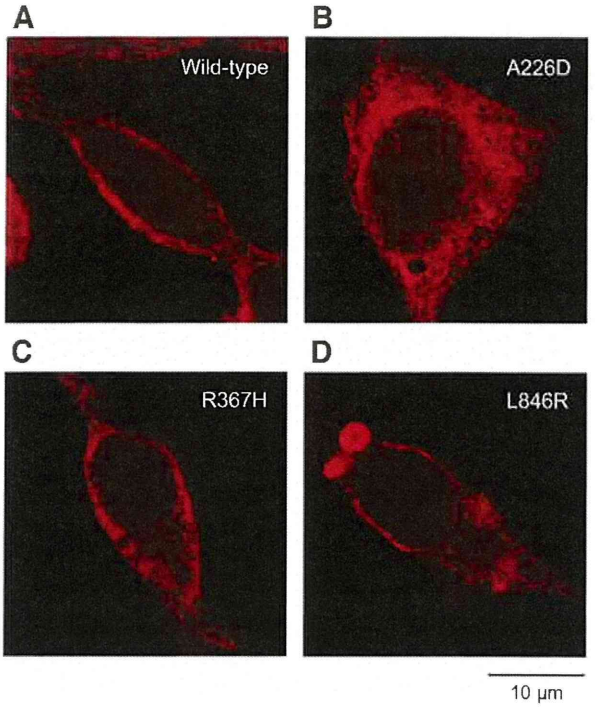

Figure 4. Representative confocal microscopy images. **A**, Cells expressing wild-type SCN5A channels showed marked peripheral fluorescence. **B**, Cells expressing A226D channels showed cytoplasmic fluorescence. **C** and **D**, Cells expressing R367H channels and those expressing L846R channels showed a similar fluorescence pattern to wild-type channels.

identification of 3 mutations in 3 unrelated probands who shared similar clinical phenotypes and the loss of sodium channel function effects in heterologous expression systems in all of the mutant channels.

Although our findings suggest that loss of sodium channel function plays a role in idiopathic ventricular fibrillation associated with early repolarization, the mechanisms of early repolarization are not understood well. In wedge preparations of canine ventricles, early repolarization results from increased action potential notches at the ventricular epicardium by either a decrease in inward currents or an increase in outward currents.[31] A mutation in *KCNJ8*, which encodes the ATP-sensitive potassium channel, recently has been identified in idiopathic ventricular fibrillation associated with early repolarization.[11] The *KCNJ8* mutation has shown gain-of-function effects in ATP-sensitive potassium channels in heterologous expression studies,[14] and augmentation of ATP-sensitive potassium currents results in the development of ventricular fibrillation in wedge preparations.[32] Decreased calcium currents also have been proposed as a mechanism for idiopathic ventricular fibrillation associated with early repolarization.[33] Mutations in L-type calcium channel genes, including *CACNA1C*, *CACNB2B*, and *CACNA2D1*, recently have been identified; however, functional studies are not yet available.[12] Our findings that mutant *SCN5A* channels displayed loss of sodium channel function, resulting in a decrease of inward currents, are consistent with findings in prior studies and with the proposed mechanism.[11,12,14,33]

In this study, heart rate and cardiac conduction were slower in patients with idiopathic ventricular fibrillation than in healthy controls. Furthermore, His-ventricular interval was prolonged in all of the patients carrying an *SCN5A* mutation. Reductions in heart rate and conduction may result from underlying electrophysiological abnormalities in idiopathic ventricular fibrillation. In addition to the maintenance of the action potential dome, normal impulse generation and propagation are dependent critically on normal sodium channel function,[34] and reductions in heart rate and conduction we observed here can be partially explained by loss-of-function mutations in *SCN5A*. Viskin et al initially reported the association of short QT interval with idiopathic ventricular fibrillation,[35] and the recent study also showed that corrected QT interval is shorter in idiopathic ventricular fibrillation patients with early repolarization than those without early repolarization.[5] In this study, corrected QT interval was shorter in patients with idiopathic ventricular fibrillation than in healthy controls, in line with the previous findings.[5,35] Furthermore, we have previously reported that early repolarization is frequently found in patients with short QT syndrome.[18] There may be the association between short QT interval and early repolarization, although the mechanism is unknown.

Idiopathic ventricular fibrillation associated with early repolarization and Brugada syndrome characterized by J-point/ST-segment elevation in the right precordial leads share genetic, clinical, and pharmacological characteristics.[5,8,12,17,25,33,36–41] Rare variants in genes encoding L-type calcium channel and ATP-sensitive potassium channel have been associated with both diseases.[12,14,36] Defects in *SCN5A* are responsible for Brugada syndrome, and we found that mutations in *SCN5A* were possible causative genetic factors in idiopathic ventricular fibrillation associated with early repolarization. Furthermore, an R367H *SCN5A* mutation identified in this study also has been reported in a family affected by Brugada syndrome.[37] However, the mechanism by which loss of sodium channel function results in either Brugada syndrome or idiopathic ventricular fibrillation associated with early repolarization is unknown, similar to that in other arrhythmia phenotypes caused by loss of function mutations in *SCN5A*, the so called cardiac sodium channelopathies.[42] There may be other genetic or environmental factors that modify the clinical phenotype. Although the association of inferolateral early repolarization with idiopathic ventricular fibrillation has been initially reported,[5] early repolarization in the right precordial leads, where Brugada type electrocardiograms can be seen, also has been associated with idiopathic ventricular fibrillation.[8,25] In this study, 2 of the 3 patients carrying an *SCN5A* mutation showed J-point elevation in the right precordial leads, but did not show diagnostic Brugada type ST-segment elevations in multiple ECG recordings even after sodium channel blocker challenge. Sinus node dysfunction and conduction disorders often are seen in Brugada syndrome, and we observed similar electrocardiographic characteristics in idiopathic ventricular fibrillation.[17,25] Bradycardia-dependent augmentation of J-point amplitude has been reported in both diseases and we observed similar changes of J-wave in a patient carrying *SCN5A* mutation.[43,44] The recent studies have shown that early repolarization is found in 14 to 24% of patients with Brugada syndrome, and that early repolarization is associated with the increased risk of arrhythmia events,[12,45] although the role of early repolarization in Brugada syndrome is not clear. The electrocardiographic manifestations of Brugada syndrome may be unmasked or augmented by sodium channel blockers.[17,25] In our present and prior studies, the administration of sodium channel blockers resulted in the augmentation of J-point amplitude or development of ventricular fibrillation in patients with idiopathic ventricular fibrillation.[46] The efficacy of isoproterenol and quinidine also is common in both diseases.[8,17,25,38–41]

In conclusion, we have shown reductions in heart rate and cardiac conduction in patients with idiopathic ventricular fibrillation associated with early repolarization. We identified *SCN5A* mutations in patients with idiopathic ventricular fibrillation and showed that mutant channels did not generate any currents. These findings implicate that *SCN5A* is a disease gene for idiopathic ventricular fibrillation associated with early repolarization, and that it plays a role in the electrocardiographic characteristics of idiopathic ventricular fibrillation, at least in part.

Acknowledgments

We thank Shigenori Terada at Akita University and Yoko Yanagida at Miyazaki Hospital for their assistance in performing this work.

Sources of Funding

This work was supported by grants from Ministry of Health, Labor, and Welfare of Japan (2010-145); Ministry of Education, Culture, Sports, Science and Technology, Japan (2010-22790696), and Grant-in-Aid for Scientific Research on Innovative Areas (HD Physiology) 22136007 (NM); Takeda Science Foundation 2010; and Japan Heart Foundation/Novartis Grant for Research Award on Molecular and Cellular Cardiology 2010.

References

1. Klatsky AL, Oehm R, Cooper RA, Udaltsova N, Armstrong MA. The early repolarization normal variant electrocardiogram: correlates and consequences. *Am J Med.* 2003;115:171–177.
2. Osborn JJ. Experimental hypothermia; respiratory and blood pH changes in relation to cardiac function. *Am J Physiol.* 1953;175:389–398.
3. Maruyama M, Atarashi H, Ino T, Kishida H. Osborn waves associated with ventricular fibrillation in a patient with vasospastic angina. *J Cardiovasc Electrophysiol.* 2002;13:486–489.
4. Shinde R, Shinde S, Makhale C, Grant P, Sathe S, Durairaj M, Lokhandwala Y, Di Diego J, Antzelevitch C. Occurrence of "J waves" in 12-lead ECG as a marker of acute ischemia and their cellular basis. *Pacing Clin Electrophysiol.* 2007;30:817–819.
5. Haissaguerre M, Derval N, Sacher F, Jesel L, Deisenhofer I, de Roy L, Pasquie JL, Nogami A, Babuty D, Yli-Mayry S, De Chillou C, Scanu P, Mabo P, Matsuo S, Probst V, Le Scouarnec S, Defaye P, Schlaepfer J, Rostock T, Lacroix D, Lamaison D, Lavergne T, Aizawa Y, Englund A, Anselme F, O'Neill M, Hocini M, Lim KT, Knecht S, Veenhuyzen GD, Bordachar P, Chauvin M, Jais P, Coureau G, Chene G, Klein GJ, Clementy J. Sudden cardiac arrest associated with early repolarization. *N Engl J Med.* 2008;358:2016–2023.
6. Rosso R, Kogan E, Belhassen B, Rozovski U, Scheinman MM, Zeltser D, Halkin A, Steinvil A, Heller K, Glikson M, Katz A, Viskin S. J-point elevation in survivors of primary ventricular fibrillation and matched control subjects: incidence and clinical significance. *J Am Coll Cardiol.* 2008;52:1231–1238.
7. Tikkanen JT, Anttonen O, Junttila MJ, Aro AL, Kerola T, Rissanen HA, Reunanen A, Huikuri HV. Long-term outcome associated with early repolarization on electrocardiography. *N Engl J Med.* 2009;361:2529–2537.